Title
Chemical stimuli override a temperature-dependent morphological program by reprogramming the transcriptome of a fungal pathogen

Author
Assa, Dror

Publication Date
2022

Peer reviewed|Thesis/dissertation

Chemical stimuli override a temperature-dependent morphological program by reprogramming the transcriptome of a fungal pathogen

by
Dror Assa

DISSERTATION
Submitted in partial satisfaction of the requirements for degree of
DOCTOR OF PHILOSOPHY

in

Biomedical Sciences

in the

GRADUATE DIVISION
of the
UNIVERSITY OF CALIFORNIA, SAN FRANCISCO

Approved:

DocuSigned by:
Suzanne Noble
816766EC3B434F2...
Suzanne Noble
Chair

DocuSigned by:
Anita Sil
Anita Sil

DocuSigned by:
Alexander Johnson
Alexander Johnson

DocuSigned by:
Jonathan Weissman
E2C110A57BC64CD...
Jonathan Weissman

Committee Members

To chosen and biological families, for unconditional love and support.

Acknowledgements

Firstly, I would like to thank my advisor, Anita Sil, for her guidance and support throughout graduate school. She has been a mentor and a role model, and I am grateful to have had her in my corner, especially at times when I felt at my lowest.

I am also thankful for my thesis committee members – Suzanne Noble, Alexander Johnson, and Jonathan Weissman, who provided important and relevant advice during my years at UCSF.

I would like to thank my lab family, past and present, who supported me in research and in life. You have made this journey worthwhile, and I hope our friendship will continue to thrive long after I graduate. I was fortunate to have found great mentors in the lab: Sinem Beyhan, Lauren Rodriguez, Bastian Joehnk, and Mark Voorhies, to name a few – this research would simply not have been possible without their mentorship and support. I also owe a great debt of gratitude to the rest of the lab, and especially Allison, Sarah, Rosa, Dinara, Bevin, Anna, Nebat, Christina, Murat, and Janey, for many fruitful scientific discussions, laughs, and life advice. You truly made the long way to a PhD not just bearable, but actually fun.

I want to thank the many friends I have made at UCSF – and especially Dan, Ramiro, Nate, Francesca, John, and Mike, for many heart-to-hearts over coffee and a pastry, or drinks, or even just a brisk walk. You provided me with mental health and scientific advice at once, and were always there when I needed you (and that was often).

I would also like to thank my mother, Mati. She has sacrificed so much to let me go on this great adventure – It is not easy to support your only child when they decide to move across the globe. Her unconditional love and belief in my capabilities, even when I have my doubts, will never cease to inspire me.

And last but certainly not least, to my husband Darwin: you have truly been my rock and safe haven for all of those years. I simply could not have done it without your patience and belief. I love you, and I thank you for everything.

Contributions

The work described in this dissertation was done under the direct supervision and guidance of Dr. Anita Sil.

The data and text from chapters 1-3 and the Materials and Methods are adapted from the following manuscript, which has been submitted to *mBio:* Assa D, Voorhies M, and Sil A. Chemical stimuli override a temperature-dependent morphological program by reprogramming the transcriptome of a fungal pathogen.

Chemical stimuli override a temperature-dependent morphological program by reprogramming the transcriptome of a fungal pathogen

Dror Assa

Abstract

The human fungal pathogen *Histoplasma capsulatum* changes its morphology in response to temperature. At 37°C it grows as a budding yeast whereas at room temperature it transitions to hyphal growth. Prior work has demonstrated that 15-20% of transcripts are temperature-regulated, and that transcription factors (TFs) Ryp1-4 are necessary to establish yeast growth. However, little is known about transcriptional regulators of the hyphal program. To identify TFs that regulate filamentation, we utilize chemical inducers of hyphal growth. We show that addition of cAMP analogs or an inhibitor of cAMP breakdown overrides yeast morphology, yielding inappropriate hyphal growth at 37°C. Additionally, butyrate supplementation triggers hyphal growth at 37°C. Transcriptional profiling of cultures filamenting in response to cAMP or butyrate reveals that a limited set of genes respond to cAMP while butyrate dysregulates a larger set. Comparison of these profiles to previous temperature- or morphology-regulated gene sets identifies a small set of morphology-specific transcripts. This set contains 9 TFs of which we characterized three, *STU1*, *FBC1*, and *PAC2*, whose orthologs regulate development in other fungi. We found that each of these TFs is individually dispensable for room-temperature (RT) induced filamentation but each is required for other aspects of RT development. *FBC1* and *PAC2*, but not *STU1*, are necessary for filamentation in response to cAMP at 37°C. Ectopic expression of each of these TFs is sufficient to induce filamentation at 37°C. Finally, *PAC2*

induction of filamentation at 37°C is dependent on *STU1*, suggesting these TFs form a regulatory circuit that, when activated at RT, promotes the hyphal program.

Table of Contents

List of Figures

List of Tables

Chapter 1 – Introduction

Histoplasma is a thermally dimorphic fungus

The fungal kingdom only composes ~2% of the Earth's biomass (Bar-On et al., 2018), but represents one of the most diverse organism groups by both form as well as function. Fungi are heterotrophs, meaning they acquire organic carbon synthesized by other organisms. Many fungi acquire this organic carbon by growing on plant and animal matter that is decomposing, but some fungi are also capable of infecting living plants or animals to obtain that carbon. In addition, the fungal kingdom can be divided into different categories based on cellular morphology. *E.g.,* some multi-cellular growth as hyphae, while others grow as unicellular yeast-shaped cells. However, there is a category of fungi that can switch between both morphologies. Thermally dimorphic fungi have developed the ability to thrive in diverse conditions, growing as hyphae at ambient temperatures and at room temperature (RT) in the laboratory, but switching to a different growth form (commonly unicellular yeast) at mammalian body temperature (37°C in the laboratory), causing an infection (a mycosis). Understanding how dimorphic fungi are able to switch between environmental growth and host growth form will allow us to develop better treatments for the illnesses they cause.

Histoplasma capsulatum is one such thermally dimorphic fungus that grows as sporulating hyphae in the soil. The spores are easily aerosolized, and upon inhalation by mammals, get engulfed by lung-resident macrophages. The spores then change their cellular shape and gene expression program to germinate into virulent yeast cells in response to mammalian body temperature. This transition to yeast cells can result in an acute pulmonary infection known as histoplasmosis (Pfaller and Diekema, 2010; Araúz and Papineni, 2021). The complex process of morphologic differentiation requires the ability to integrate signals on a

molecular level and convert those signals into transcriptional, translational and biochemical changes that orchestrate the transition from one growth form to another.

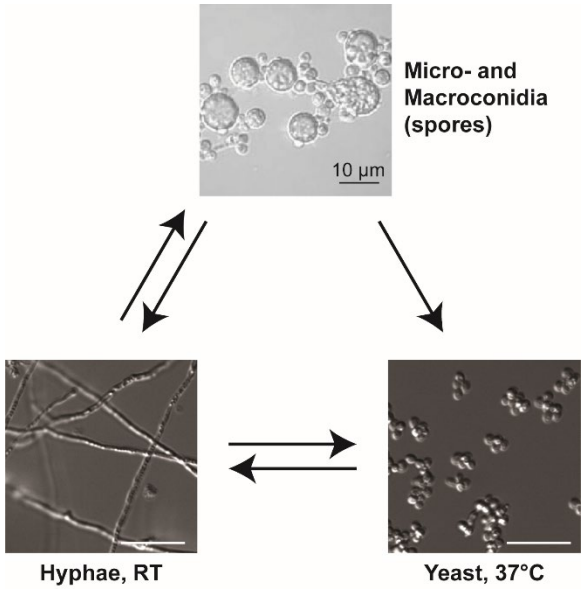

Figure 1.1. The different morphologies of *Histoplasma.*
Histoplasma grows as hyphae in the soil, producing two kinds of spores: micro- and macroconidia. At ambient temperature, the spores can germinate into hyphae. However, when these spores are aerosolized and inhaled by a mammal, the elevated body temperature causes germination into a yeast morphology. In the lab, changing the temperature is sufficient to switch between hyphal-phase growth (at RT) and yeast phase growth (at 37°C). Scale bar denotes 10 µm; Source for conidia image: Inglis et al., 2013.

Regulation of morphology in *Histoplasma*

The molecular basis of *Histoplasma's* ability to transition between morphologies has been at the focus of many studies over the past few decades. One of the most important insights from these studies is that 15-20% of transcripts in *Histoplasma* are regulated by temperature (Gilmore et al., 2015; Beyhan et al., 2013; Edwards et al., 2013), indicating that the switch between yeast and hyphal morphologies correlates with a substantial remodeling of the transcriptome. Specific functions, such as virulence, iron acquisition, and cell wall modification are correlated with 37°C and yeast-phase growth, whereas the hyphal growth form that dominates at room temperature promotes the expression of enzymes such as tyrosinases, cytochrome p450s, oxidoreductases, and peroxidases. Additionally, the abundance of

Histoplasma transcripts encoding 18 putative transcription factors is increased in hyphae compared to yeast, whereas only 6 transcripts encoding putative transcription factors are differentially abundant in yeast cells (Gilmore et al., 2015).

Forward genetic screens have been instrumental in finding regulators of morphology in *Histoplasma*. *Agrobacterium tumefaciens*-assisted mutagenesis screens have identified Drk1, a hybrid histidine kinase orthologous to *Candida albicans* Nik1 (Defosse et al., 2015), which is necessary for yeast morphology (Nemecek et al., 2006), and 3 transcription factors that are also required for yeast phase (RYP) growth: Ryp1, a WOPR family transcription factor orthologous to *Candida albicans* Wor1 (Nguyen and Sil, 2008), and Ryp2/3, both velvet family transcription factors orthologous to *Aspergillus* VosA and VelB, respectively (Webster and Sil, 2008). Follow up studies also identified an additional transcription factor required for yeast phase growth, Ryp4, a Zn(II)2Cys6 zinc binuclear cluster domain protein (Beyhan et al., 2013). Chromatin immunoprecipitation (ChIP) and microarray analysis revealed that Ryp1, 2, 3, and 4 also associate with the promoters of Ryp1, 2, and 4, forming a temperature-responsive, interconnected regulatory network. Interestingly, transcriptional profiling of *ryp* mutants at 37°C reveals similar transcriptomes to that of wild-type hyphae at RT, indicating that the Ryp transcription factors are master regulators of the yeast-phase program and couple the transcriptional response to temperature with morphology (Beyhan et al., 2013).

On the hyphal side, Gilmore *et al.* showed that inappropriate expression of the transcription factor Wet1 is sufficient to cause filamentous growth at 37°C in *Histoplasma* (Gilmore et al., 2015). Wet1 is orthologous to wetA in *aspergillus*, which regulates the late stages of asexual spore production (Sewall et al., 1990). More recently, Rodriguez *et al.* reported that expression of the APSES-family transcription factor Stu1, which is orthologous to StuA in *Aspergillus* and Enhanced Filamentous Growth 1 (Efg1) in *C. albicans*, is also sufficient to trigger inappropriate filamentous growth at 37°C in *Histoplasma* (Rodriguez et al., 2019). On the other hand, Longo *et al*. showed that using RNA interference to target Stu1 resulted in

decreased formation of aerial hyphae on plates (Longo et al., 2018). StuA coordinates conidiophore formation in *Aspergilli* (Sheppard et al., 2005; Dutton et al., 1997), and Efg1 is necessary for filamentous growth in *C. albicans* (reviewed in (Glazier, 2022)).

In addition to differences between the transcriptomes of hyphae and yeast, other mechanisms also participate in regulating morphology in response to temperature. Using RNA sequencing analysis, Gilmore *et al.* has revealed that in ~2% of the transcriptome, transcriptional start site is differential between yeast and hyphae (Gilmore et al., 2015). Moreover, ribosome profiling suggests another layer of regulation, in which transcripts exhibit differential translational efficiency, likely altering protein levels independently of transcript abundance. In particular, a small subset of interesting transcripts is regulated by both of these processes. This group includes the *WET1* transcript, which is both longer in the yeast phase exhibits decreased translational efficiency in yeast. Conversely, the *RYP2* transcript is both longer and less efficiently translated in the hyphal phase (Gilmore et al., 2015). Together these findings show that multiple, levels of intricate regulation control gene expression and morphology in *Histoplasma*, likely speaking to the importance of the morphology switch in *Histoplasma* biology.

The cAMP-PKA pathway in fungi

In this study we examine the relationship between transcription, *Histoplasma* hyphal formation, and the cAMP/protein kinase A (PKA) pathway, which is a central and conserved signaling pathway in all eukaryotes. In fungi, the cAMP-PKA pathway is critical for numerous cellular processes, including regulation of carbon utilization, mating, morphology, stress response, and virulence. The cAMP-PKA pathway has been the subject of extensive mechanistic research in *Saccharomyces cerevisiae* (reviewed in (Conrad et al., 2014; Creamer et al., 2022; Fuller and Rhodes, 2012)). In this organism, fermentable carbon sources such as glucose are sensed by several pathways that lead to the activation of adenylate cyclase, which

synthesizes cAMP from ATP. cAMP then binds the regulatory subunits of PKA, releasing the catalytically active subunits to phosphorylate target proteins that facilitate numerous biological functions.

One of the main roles of the cAMP-PKA pathway in *S. cerevisiae* is to allow rapid response to stress. In non-stress conditions, the transcription factors Msn2/4p are phosphorylated by PKA, preventing them from entering the cell nucleus (de Wever et al., 2005). Various stress signals inactivate PKA rapidly and cause the dephosphorylation of Msn2/4p, allowing it to access the cell nucleus, leading to the induction of the environmental stress response (Gasch et al., 2000; Smith et al., 1998; Boy-Marcotte et al., 1998; Görner et al., 1998; Garreau et al., 2000). Other outcomes of PKA inactivation include induction of gluconeogenesis, respiration, and alternative energy source utilization pathways and repression of cell division and ribosomal biogenesis pathways, which all aid in adaptation to environmental stressors (Conway et al., 2012; Jorgensen et al., 2004). Additionally, the cAMP-PKA pathway regulates pseudohyphal growth in *Saccharomyces* growth by activating the transcription factor Flo8p (Pan and Heitman, 1999, 2002).

Signaling through the cAMP-PKA pathway is central to morphological and developmental decisions, with implications for virulence in multiple pathogenic fungi. In *Candida* species, the cAMP-PKA pathway integrates signals such as environmental pH, N-acetylglucosamine (GlcNAc), and the presence of serum in growth media, and, depending on specific contexts, positively regulates white-opaque switching or the transition to hyphal growth, mediated by the activation of Efg1 (Rocha et al., 2001; Bockmühl and Ernst, 2001; Parrino et al., 2017; Min et al., 2021; Saputo et al., 2014; Cao et al., 2017; Stoldt et al., 1997; Sonneborn et al., 2000). The activity of the cAMP-PKA pathway is also necessary for the expression of virulence genes in *C. albicans* (Klengel et al., 2005; Cao et al., 2017; Harcus et al., 2004). In *Aspergillus* spp., sensing of signals such as glucose by hetero-trimeric G-protein leads to activation of the cAMP-PKA pathway and influences the transition between hyphae and spore

morphology, inducing spore germination, inhibiting sporulation and coordinating the synthesis of secondary metabolites (Fillinger et al., 2002; Liebmann et al., 2003; Lafon et al., 2005; Fuller et al., 2011; Liebmann et al., 2004; Shimizu and Keller, 2001).

The cAMP-PKA pathway also plays an important role in cell morphology regulation in thermally dimorphic fungi. Intracellular and extracellular cAMP levels rise when *Histoplasma* G217B yeast (growing at 37°C) are shifted to room temperature, concurrent with the formation of hyphae (Medoff et al., 1981). These data suggest a correlation between cAMP accumulation and filamentation. Moreover, addition of the stable cAMP analog dibutyryl-cAMP (dbcAMP) to *Histoplasma* cultures growing at 37°C promotes filamentous growth (Maresca et al., 1977; Sacco et al., 1981; Medoff et al., 1981). Similarly, in the closely related dimorphic fungi *Paracoccidioides brasiliensis* and *Blastomyces dermatitidis*, exogenous cAMP delays the transition from hyphae to yeast (45, 46). However, the underlying molecular mechanisms of filamentation induced by exogenous activation of the cAMP pathway in thermally dimorphic fungi have not been examined.

In this study, we used transcriptome profiling of *Histoplasma* to further understand the molecular events that occur upon chemical induction of filamentation. By comparing the transcriptome induced by addition of cAMP analogs to the room temperature-induced transcriptome, we identified groups of transcripts whose accumulation is closely associated with yeast or hyphal morphologies. Using these data, we focused on 3 transcription factors that have been shown to regulate morphology and development in other organisms and showed that they are capable of driving a hyphal program in *Histoplasma.*

Chapter 2 – Morphological and transcriptional characterization of the response to cAMP analogs and butyrate in *Histoplasma*

cAMP analogs drive inappropriate filamentation at 37°C

As described in the introduction, previous studies have demonstrated that addition of exogenous cAMP, in the form of the cell-permeable analog dbcAMP, induces filamentous growth in *Histoplasma capsulatum* (Maresca et al., 1977). We hypothesized that addition of cAMP leads to molecular changes that override the normal transcriptional program at 37°C, which is governed by the activity of the transcription factors Ryp1-4, and that by identifying these molecular changes we will gain better understanding of factors that contribute to filamentation at room temperature.

To characterize the effect of dbcAMP on *Histoplasma* growth, we added dbcAMP to early-log phase G217B and the derived uracil-auxotrophic mutant G217B*ura5* (WU15) cultures growing at 37°C in HMM containing glucose or N-acetylglucosamine (HMM+GlcNAc) as main carbon sources. Our previous work showed that GlcNAc stimulates hyphal growth upon shift from 37°C to RT (Gilmore et al., 2013). While no morphological difference was observed after one day (data not shown), within 2 days a noticeable increase in filamentous growth occurred in cultures growing in HMM+GlcNAc and treated with dbcAMP compared to the vehicle (water). In contrast, 10 mM dbcAMP did not affect the morphology of yeast cultures in HMM containing only glucose (**Fig. 2.1B**). Hyphal growth was even more evident by the third day after dbcAMP addition (**Fig. 2.2A**). The extent to which dbcAMP promotes filamentation was concentration-dependent: a visible increase in filamentous growth could be observed in cultures with as little as 1.25 mM dbcAMP (**Fig. 2.2B**). Addition of dbcAMP to solid media (HMM agarose containing GlcNAc) also strongly favored filamentous growth at 37°C (**Fig. 2.1C**).

We next wanted to test whether other means of increasing cAMP levels had a similar effect on hyphal formation. Normally cAMP is broken down within the cell by the action of

phosphodiesterases. We attempted to raise cAMP levels by adding cAMP sodium salt or the phosphodiesterase inhibitor IBMX. Whereas 25 mM cAMP had a negligible effect on morphology on its own, the addition of 1.25 mM IBMX was sufficient to trigger filamentation within 2 days (**Fig. 2.1D**). Adding both cAMP and IBMX had a stronger filamentation effect, suggesting that minimizing the breakdown of exogenous cAMP by inhibiting phosphodiesterase activity may cause a net increase in cAMP levels that promotes filamentation. Furthermore, adding 8-(4-chlorophenylthio)adenosine 3',5'-cyclic monophosphate (8-CPT-cAMP), an alternative cAMP analog, also promoted robust filamentation (**Fig. 2.1E**). Taken together, these data confirm that exogenously added cAMP overrides yeast phase growth and promotes filamentation at 37°C.

The transition from yeast to hyphae in response to temperature shift is less robust in glucose relative to GlcNAc (Gilmore et al., 2013). To determine if the addition of exogenous cAMP addition promotes filamentation in response to temperature shift in glucose, where the transition is asynchronous and inefficient, we added 10 mM dbcAMP to cultures shifted from 37°C to RT in glucose-containing media. We observed a subtle (**Fig. 2.1F**) but statistically significant (**Fig. 2.1G**) increase in elongated cells and filamentous structures in liquid culture by day 7 after shift in the presence of dbcAMP.

Since dbcAMP hydrolysis can release butyrate into the growth media, we also investigated the effect of adding sodium butyrate on its own to *Histoplasma* growth media. In the presence of GlcNAc, butyrate strongly induced filamentation within 2 days; however, the effect of butyrate was much more potent than dbcAMP. For example, 10 mM dbcAMP stimulated robust filamentation by day 2 (**Fig. 2.1B**), but yeast cells were still present. In contrast, 5 mM butyrate stimulated complete hyphal transformation with no yeast cells remaining in the cultures (**Fig. 2.1H**). We were surprised that the hydrolysis product had greater filamentation-inducing activity than the cAMP analog itself. Nevertheless, the similar activity of 8-CPT-cAMP and of cAMP, with the addition of a phosphodiesterase inhibitor, neither of which cannot be hydrolyzed

to release butyrate, suggests that cAMP itself is an inducer of filamentation. Our serendipitous discovery of potent activity for butyrate yielded an additional chemical tool to probe the transcriptional correlates of filamentation.

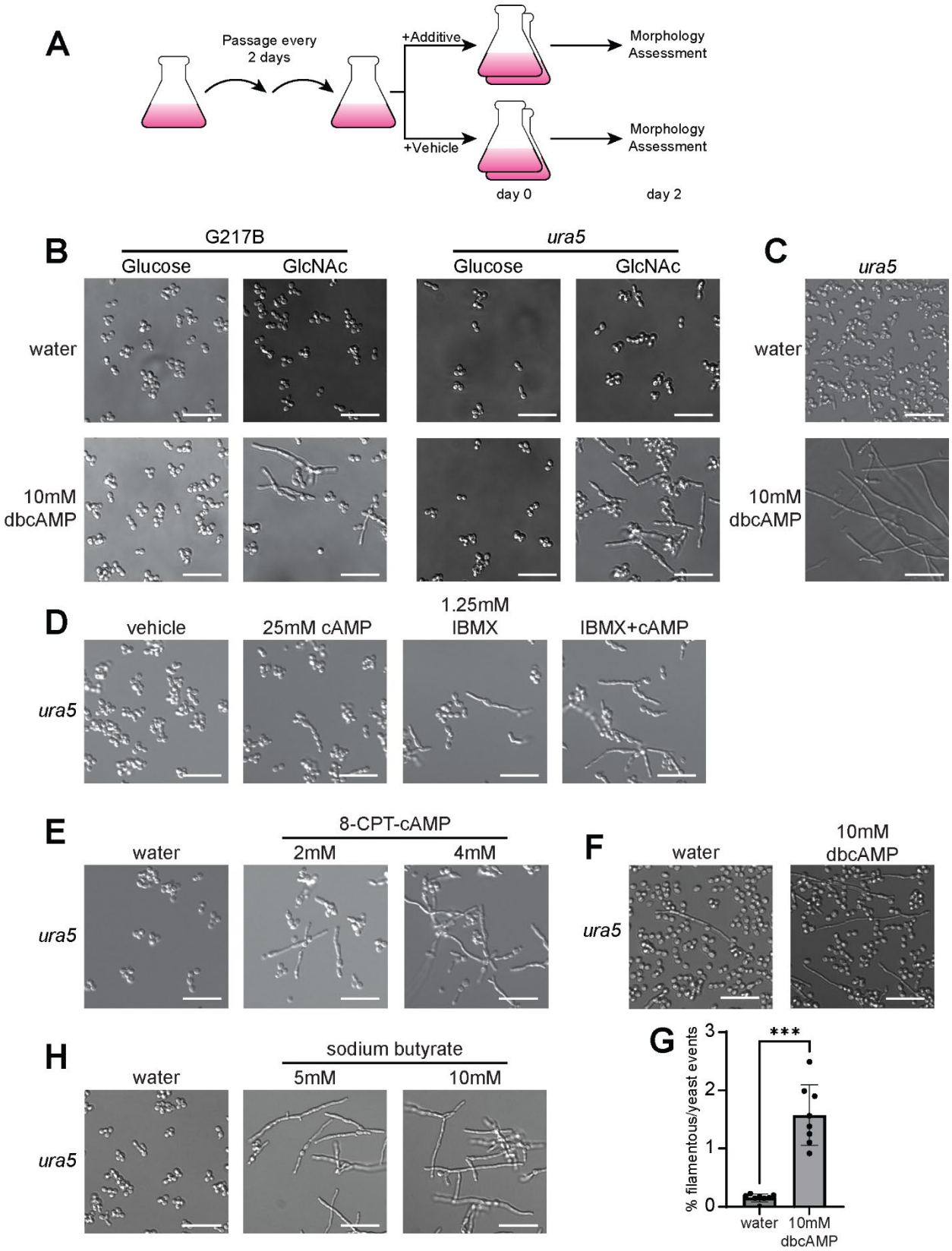
A
Passage every 2 days
+Additive
+Vehicle
Morphology Assessment
Morphology Assessment
day 0
day 2
B
G217B
ura5
Glucose
GlcNAc
Glucose
GlcNAc
water
10mM dbcAMP
C
ura5
water
10mM dbcAMP
D
vehicle
25mM cAMP
1.25mM IBMX
IBMX+cAMP
ura5
E
8-CPT-cAMP
water
2mM
4mM
ura5
F
water
10mM dbcAMP
ura5
H
sodium butyrate
water
5mM
10mM
ura5
G
% filamentous/yeast events
***
water
10mM dbcAMP

Figure 2.1. Exogenous cAMP promotes filamentous growth at 37°C.
(A) Schematic outline of experiments testing the response of *Histoplasma* to chemical additives. (B) Cell morphology of G217B and G217B*ura5 Histoplasma* after 2 days of growth at 37°C in liquid HMM containing glucose or GlcNAc with or without 10mM dbcAMP. (C) Cell morphology of G217B*ura5 Histoplasma* after 8 days of growth on HMM-agarose plates containing GlcNAc, with or without 10mM dbcAMP, at 37°C. (D) Cell morphology of G217B*ura5 Histoplasma* after 2 days of growth at 37°C in liquid HMM containing GlcNAc with 1.25mM IBMX, 25mM cAMP, IBMX+cAMP, or water as vehicle control. (E) Cell morphology of G217B*ura5 Histoplasma* after 2 days of growth at 37°C in liquid HMM containing GlcNAc with 4mM or 2mM 8-CPT-cAMP, or water as vehicle control. (F) Cell morphology of G217B*ura5 Histoplasma* after 7 days of growth at RT in liquid HMM containing glucose with or without 10mM dbcAMP. (G) Quantification of filamentation after 7 days at RT in liquid HMM containing glucose with or without 10mM dbcAMP; N > 243 events. (H) Cell morphology of G217B*ura5 Histoplasma* after 2 days of growth at 37°C in liquid HMM containing GlcNAc with 5mM or 10mM sodium butyrate, or water as vehicle. Scale bar denotes 10 μm; *** $p < 0.001$, Wilcoxon rank-sum test.

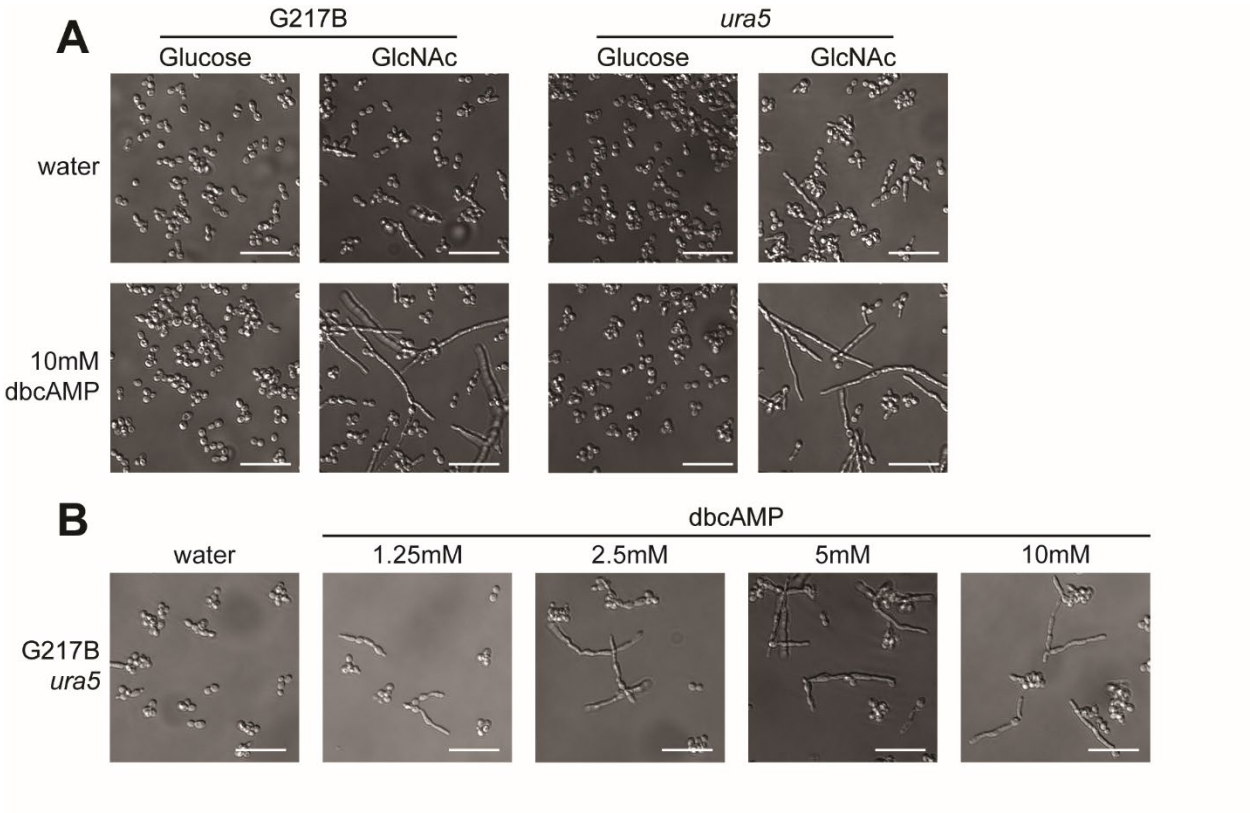

Figure 2.2. dbcAMP promotes filamentous growth at 37°C.
(A) Cell morphology of G217B and G217B*ura5 Histoplasma* after 3 days of growth at 37°C in liquid HMM containing glucose or GlcNAc with or without 10mM dbcAMP. (B) Cell morphology of G217B*ura5 Histoplasma* after 2 days of growth at 37°C in liquid HMM containing GlcNAc with various concentrations of dbcAMP. Scale bar denotes 10 μm.

cAMP analogs and butyrate stimulate robust transcriptional changes

To further understand the molecules and pathways that mediate filamentation after addition of cAMP analogs, we performed transcriptional profiling of G217B*ura5 Histoplasma* cultures grown in HMM+GlcNAc media at 37°C with addition of 10 mM dbcAMP, 4 mM 8-CPT-cAMP, 5mM butyrate, or water as vehicle control. Each of these additions stimulated filamentation compared to the water control (**Fig. 2.3A**). We found that 721 or 1083 transcripts were significantly up-regulated in response to dbcAMP or 8-CPT-cAMP, respectively (>1.5 fold change, FDR < 5%) and 639 or 1000 transcripts were down-regulated in response to dbcAMP or 8-CPT-cAMP, respectively. In comparison, the response to butyrate involved many genes: 2091 transcripts were up-regulated in response to butyrate, and 2383 transcripts were down-regulated.

A previous forward genetic screen for yeast-locked mutants identified SG1, a WU15-derived strain that is refractory to filamentous growth in response to acute room temperature shift (Rodriguez et al., 2019). In contrast to wild-type cells, SG1 did not filament in response to 10 mM dbcAMP at 37°C (**Fig. 2.3B**). However, SG1 did filament in response to 10 mM butyrate, albeit to a lesser extent than the wild-type strain (**Fig. 2.3C**), highlighting the differential effects of dbcAMP and butyrate addition. Given the distinct morphological response of SG1 to dbcAMP compared to wild-type *Histoplasma*, we performed a second transcriptional profiling experiment comparing the responses of G217B*ura5* and SG1 yeast to dbcAMP treatment.

The effects of cAMP analogs on the transcriptome of G217B*ura5* are highly correlated (**Fig. 2.3D**, Pearson's $r = 0.9$). In contrast, the transcriptional response to butyrate is overlapping but distinct (**Fig. 2.3E**, $r = 0.5$). The transcriptional changes due to the SG1 genotype are weakly anti-correlated to the effect of dbcAMP on G217B*ura5* (**Fig. 2.3F**, $r = -0.4$), indicating that SG1 responds differently than G217B*ura5* to cAMP analogs transcriptionally as well as morphologically. Simultaneously considering the correlations among all of the transcriptional profiles with principal components analysis (PCA) reveals a first component, representing half of

the total variance, that captures the correlated response to dbcAMP and butyrate, anticorrelated with the effects of the SG1 genotype, and a second component, representing half of the remaining variance, capturing an orthogonal response unique to butyrate (**Fig 2.3G**).

To stringently define high confidence regulons specific to yeast or hyphal morphology, we progressively gated the transcriptome on expression values that change when the cells are given a filamentation signal in a manner that is dependent on genotype (wild-type or SG1) (**Fig. 2.4**). 1270 transcripts were up-regulated (*i.e.* showed increased abundance) in response to either cAMP analog. Of these, 594 were also up-regulated in response to butyrate. Of these, 436 were also induced at RT in at least one of two previously published room temperature experiments. Of these, 207 were down-regulated (*i.e.* showed decreased abundance) in the non-filamenting SG1 mutant. Finally, 117 of these transcripts were also down in response to dbcAMP in the SG1 experiment, and we designated this set as the stringently-defined hyphal-associated set (Class 1 in **Fig. 2.5A, B**). Likewise, 1186 transcripts were down regulated in response to either cAMP analog. Of these, 842 were also down regulated in response to butyrate. Of these, 563 were also repressed at RT in at least one of the previously published room temperature experiments. Of these, 265 were up-regulated in the non-filamenting SG1 mutant. Finally, a high confidence yeast associated subset of 97 of these genes were also up in response to dbcAMP in the SG1 experiment. We designated this set as the stringently defined yeast-associated set (Class 12 in **Fig. 2.5A, C**).

The stringently defined yeast associated set includes the known virulence factors *CBP1* (Sebghati et al., 2000; Isaac et al., 2015; English et al., 2017; Azimova et al., 2022), *CATP* (Holbrook et al., 2013; Johnson et al., 2002), *ENG1* (Garfoot et al., 2016), *LDF1* (Isaac et al., 2015), and the siderophore biosynthetic genes *SID3* and *SID4* (Hwang et al., 2008). The siderophore biosynthetic cluster as a whole is more down regulated in cAMP than in butyrate, with the remaining genes in the cluster passing our significance criteria only for cAMP. More broadly, genes down regulated in response to butyrate, cAMP, and RT include the additional

virulence factor *SOD3* (Youseff et al., 2012); regulator of bud site selection *RSR1*; yeast cell wall associated enzymes *AMY3* (Marion et al., 2006) and *CTS1*/*CHS1*; and GH17/*CFP4*, a secreted yeast gene of unknown function (Chandrashekar et al., 1997; Holbrook et al., 2014). The ER chaperones *KAR2* (BiP), *LHS1*, and *CNE1* (calnexin) are likewise downregulated, as is *OCH1*, an initiator of N-linked glycosylation. This group is also enriched for genes whose promotors are bound by Ryp1 (p = 7.5e-3), Ryp2 (p = 1.7e-4), and Ryp3 (p = 7.5e-4, Benjamini-Hochberg corrected hypergeometric test), the transcription factors that drive yeast-phase growth.

In contrast, the stringently defined hyphal-associated set (Class 1 in **Fig. 2.5A, B**) includes anabolic enzymes associated with lipid and riboneogenesis, previously identified hyphal-specific factors, and a variety of signaling molecules of which nine are transcription factors. Zamith-Miranda et al have annotated 77 lipid metabolic genes in Histoplasma capsulatum G186AR (Zamith-Miranda et al., 2021), 71 of which have G217B orthologs with detectable transcripts in our data set. These genes are significantly up-regulated in butyrate vs. water (p = 1.3e-5) and to a lesser extent in cAMP vs. water (p = 4.9e-4, Wilcoxon rank-sum test). In particular, we do not observe any of the lipid metabolic genes down regulated in response to dbcAMP, only one down in response to 8-CPT-cAMP, and only three down in response to butyrate. Lipid metabolic genes upregulated only in butyrate include the ergosterol pathway. Lipid metabolic genes upregulated in class 1 include the core fatty acid synthase (FAS1 and FAS2) as well as an elongase (ELO2/GIG30). It may be that increased lipid production modulates hyphal membrane fluidity at RT and thus is coupled to the hyphal program even when filamentation is inappropriately induced at 37°C by chemical stimuli.

The reducing potential to drive fatty acid biosynthesis can be derived from isocitrate dehydrogenase or the oxidative arm of the pentose phosphate pathway (Minard et al., 1998). While isocitrate dehydrogenase (*IDH1*) is not differential in our dataset, *ZWF1*, which catalyzes the first committed step of the oxidative pentose phosphate pathway, yielding NADPH, is in

class 1. *GND1*, which catalyzes the other NADPH generating step of this pathway, is upregulated in butyrate but not cAMP. Intriguingly, *SHB17*, which catalyzes the first committed step in the non-oxidative arm of the pentose phosphate pathway is also in class 1. Therefore, these conditions are generating both reducing potential to drive fatty acid biosynthesis, via *ZWF1*, as well as riboneogenesis via *SHB17*, possibly due to increased protein synthesis to replace yeast-specific proteins with hyphal-specific proteins during the transition. While we do not detect upregulation of translational machinery in class 1, GO enrichment analysis reveals that 200 ribosome, pre-ribosome, or rRNA processing genes, as well as 28 tRNA processing genes are upregulated in butyrate (class 6). This set of 228, which is down by a median of 2.4-fold in butyrate vs. water, is also subtly down in 8-CPT-cAMP vs. water (9%) and dbcAMP (13%) and significantly distinguishable from the remainder of the transcriptome ($p < 1e-4$ in both cases, Wilcoxon rank sum test), suggesting a greater degree of protein turnover corresponding to the stronger hyphal induction in butyrate treated cells. In addition to its roles in lipid biosynthesis and riboneogenesis, we note that *Saccharomyces* null mutants of *ZWF1* require an organic sulfur source to grow (Thomas et al., 1991). Therefore, our observed hyphal-specific expression of *ZWF1* is interesting given the known cysteine auxotrophy of *Histoplasma* yeast but not hyphae (Scherr, 1957). On a related note, we see upregulation of the sulfur assimilation pathway in response to filamentation: the first and last genes (*SUL1* and *MET17A*) are in class 2, another (*MET10*) is up in butyrate, and the remainder (*MET3*, *MET14*, *MET16*, and *MET5*) are up in butyrate vs. water, cAMP vs. water, and RT/37°C but not down in SG1/G217B*ura5* (class 3). Additionally, 15 genes involved in amino acid synthesis pathways are upregulated in response to dbcAMP.

In additional to the annotated lipid genes (Zamith-Miranda et al., 2021), we note three distinct phospholipases in class 1. One phospholipase B (*PLB1*) and one phospholipase D (*PDL1*) have plausible roles in signaling. In particular, the *PLD1* homolog *SPO14* has regulatory roles in meiosis and sporulation in Saccharomyces. Edwards et al previously noted higher

expression of *PLB1* and *PLD1* in G186AR vs. G217B yeast (Edwards et al., 2013). The third phospholipase, *PLD2*, which has a conserved secretion signal sequence, is from a distinct lineage of phospholipase D toxins; consistent with toxin function, the *Coccidioides* ortholog of *PLD2* cyclizes, rather than cleaves, lipids (Lajoie and Cordes, 2015).

A number of regulatory genes are in class 1, including protein kinases *NIT5* and *HOG2*, protein phosphatase *GAC1*, and the G protein coupled receptor *gprM*. In addition, there are nine transcription factors: *ZNC1*, *YAP1*, *sclB*, *nosA*, *STU1*, *PAC2*, *FBC1*, and two TFs of unknown function (ucsf_hc.01_1.G217B.00081 and ucsf_hc.01_1.G217B.09028) (**Fig. 2.6**). In the dimorphic fungus *Yarrowia lipolytica*, Znc1 is a negative regulator of hyphal growth (Martinez-Vazquez et al., 2013), and sclB is a known developmental regulator in Aspergillus. Of 408 differential genes from RNAseq of *sclB*$^-$/WT (Thieme et al., 2018), 31 sclB-repressed and 68 sclB-induced genes have *Histoplasma* orthologs observed in our data. Class 1 contains none of the repressed and five of the induced genes; *viz*., the TFs *FBC1* and ucsf_hc.01_1.G217B.00081 and three enzymes: ucsf_hc.01_1.G217B.03634, ucsf_hc.01_1.G217B.01297, and ucsf_hc.01_1.G217B.08874. Orthologs of *nosA*, *FBC1* and *STU1* are likewise known developmental regulators in Aspergillus (Vienken and Fischer, 2006a; Miller et al., 1992; Kwon et al., 2010), and in Histoplasma *STU1* overexpression is sufficient for hyphal growth at 37°C (Rodriguez et al., 2019).

To determine if cAMP analog/butyrate addition affects known regulators of yeast-phase growth, we examined our transcriptional profiles for levels of *RYP1-4* transcripts. *RYP1* and *RYP4* transcript levels were not affected by cAMP analogs but were reduced in butyrate-treated samples; *RYP2* transcript levels were reduced in response to cAMP analogs only in one of the two experiments; and *RYP3* levels were not affected by any treatments. Since Ryp1 and Ryp2 are known to be post-transcriptionally regulated (Gilmore et al., 2015), we reasoned that cAMP and/or butyrate could affect Ryp protein levels. We performed Western blot analysis to assay the levels of the Ryp1, Ryp2, and Ryp3 proteins in cultures grown in the presence of dbcAMP,

8-CPT-cAMP, or butyrate. Ryp1 and Ryp2 protein levels appeared to be unchanged in response to these chemicals. In contrast, Ryp3 levels were reduced in response to dbcAMP and 8-CPT-cAMP and further reduced in response to butyrate (**Fig. 2.3H**). These observations suggest that a reduction in Ryp3 levels may contribute to filamentation in response to these chemical perturbations.

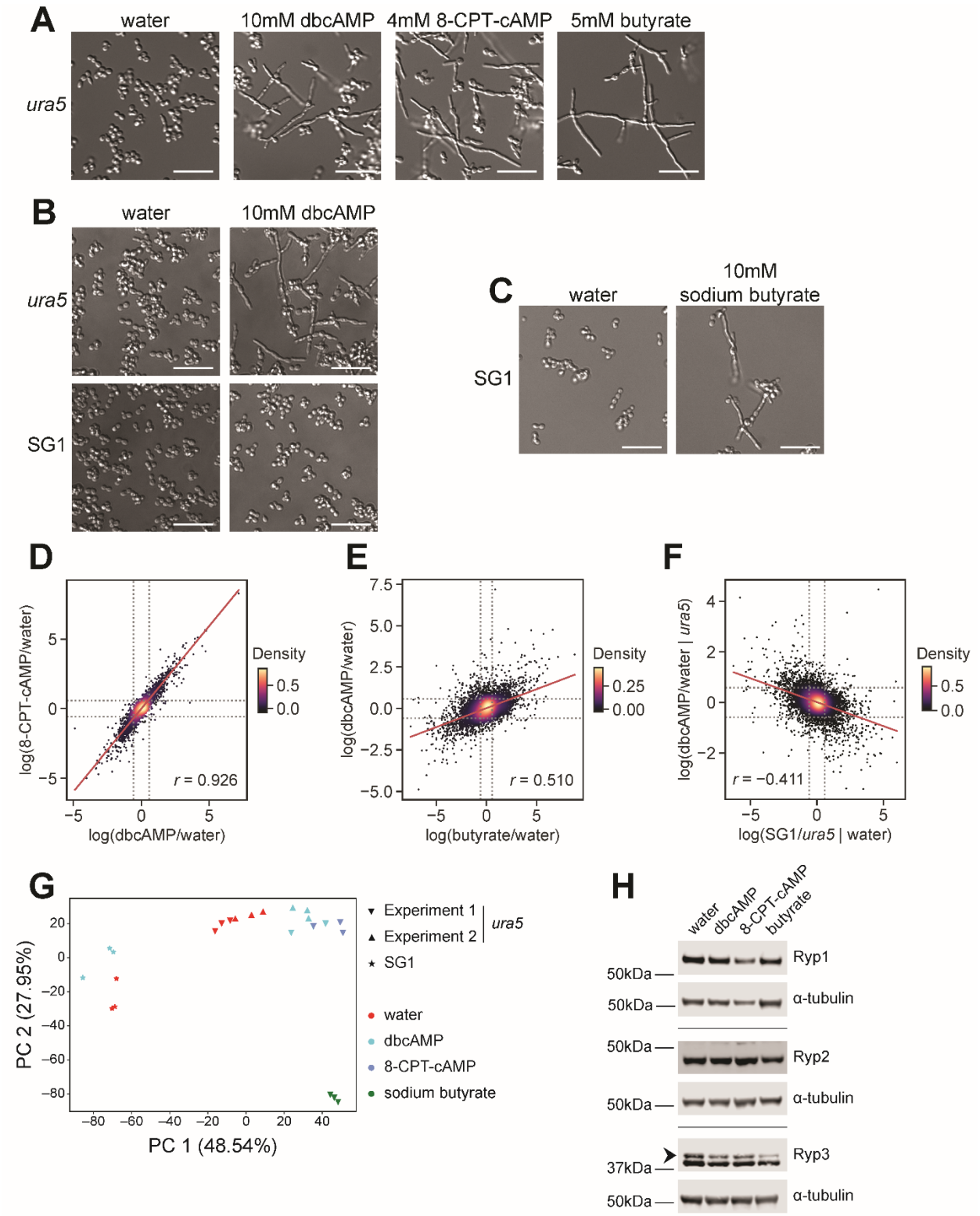
A
water
10mM dbcAMP
4mM 8-CPT-cAMP
5mM butyrate
ura5
B
water
10mM dbcAMP
ura5
SG1
C
water
10mM sodium butyrate
SG1
D
log(8-CPT-cAMP/water)
log(dbcAMP/water)
Density
0.5
0.0
r = 0.926
E
log(dbcAMP/water)
log(butyrate/water)
Density
0.25
0.00
r = 0.510
F
log(dbcAMP/water | ura5)
log(SG1/ura5 | water)
Density
0.5
0.0
r = −0.411
G
PC 2 (27.95%)
PC 1 (48.54%)
Experiment 1
Experiment 2
ura5
SG1
water
dbcAMP
8-CPT-cAMP
sodium butyrate
H
water
dbcAMP
8-CPT-cAMP
butyrate
50kDa
Ryp1
α-tubulin
Ryp2
37kDa
Ryp3

Figure 2.3. The transcriptional response to cAMP analogs and butyrate.
(A) Cell morphology of G217B*ura5 Histoplasma* after 2 days of growth at 37°C in liquid HMM containing GlcNAc with 10mM dbcAMP, 4mM 8-CPT-cAMP, 5mM butyrate, or water as vehicle control. (B) Cell morphology of G217B*ura5* and SG1 *Histoplasma* after 2 days of growth at 37°C in liquid HMM containing GlcNAc with 10mM dbcAMP or water as vehicle control. (C) Cell morphology of SG1 *Histoplasma* after 2 days of growth at 37°C in liquid HMM containing GlcNAc with 10mM sodium butyrate or water as vehicle control. (D, E) Scatter plots of $\log_2$ LIMMA-fit treatment/vehicle contrasts; dashed line indicates fold-change of $\log_2 1.5$. (F) Scatter plots of $\log_2$ LIMMA-fit contrasts for genotype (with vehicle) versus treatment (in G217B*ura5*); dashed line indicates fold-change of $\log_2 1.5$. (G) Principal component analysis (PCA) of all genes expressed in G217B*ura5* and SG1 *Histoplasma* treated with dbcAMP, 8-CPT-cAMP, sodium butyrate, or water. In parentheses: percent of total variance explained by the principal component. (H) Western blots performed on protein extracted from G217B*ura5 Histoplasma* after 2 days of growth at 37°C in liquid HMM containing GlcNAc with 10mM dbcAMP, 4mM 8-CPT-cAMP, 5mM butyrate, or water as vehicle control; arrow distinguishes Ryp3 band from known background band. Scale bar denotes 10 µm; *r*, Pearson's correlation coefficient.

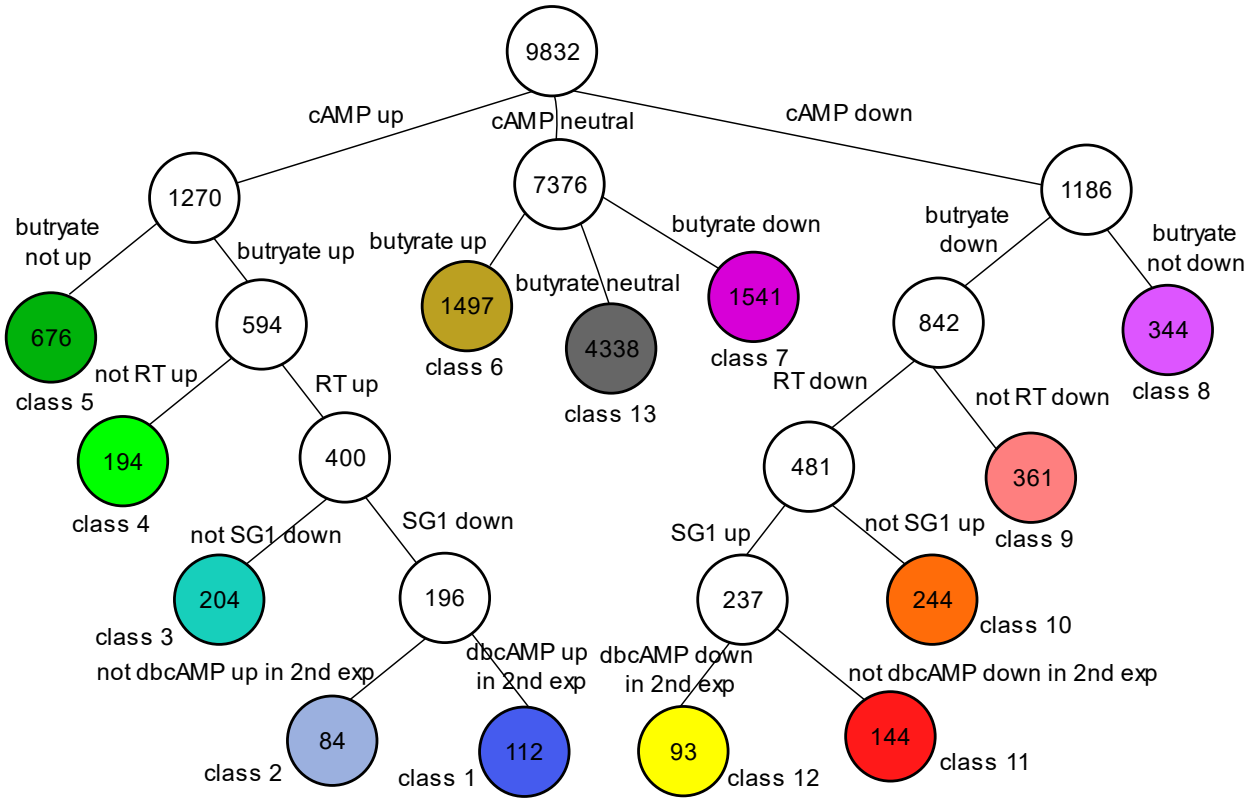

Figure 2.4. Classification of genes by expression profile.
Scheme for the classification of genes as discussed in the text and shown in **Fig. 2.5**. The top node indicates the 9832 genes observable in the expression profiling data. Edges divide each internal node into disjoint sets, with edge labels indicating the division criteria. Numbers inside nodes indicate the number of genes in the corresponding set. The colored terminal nodes indicate the final, disjoint classification spanning the 9832 observed genes.

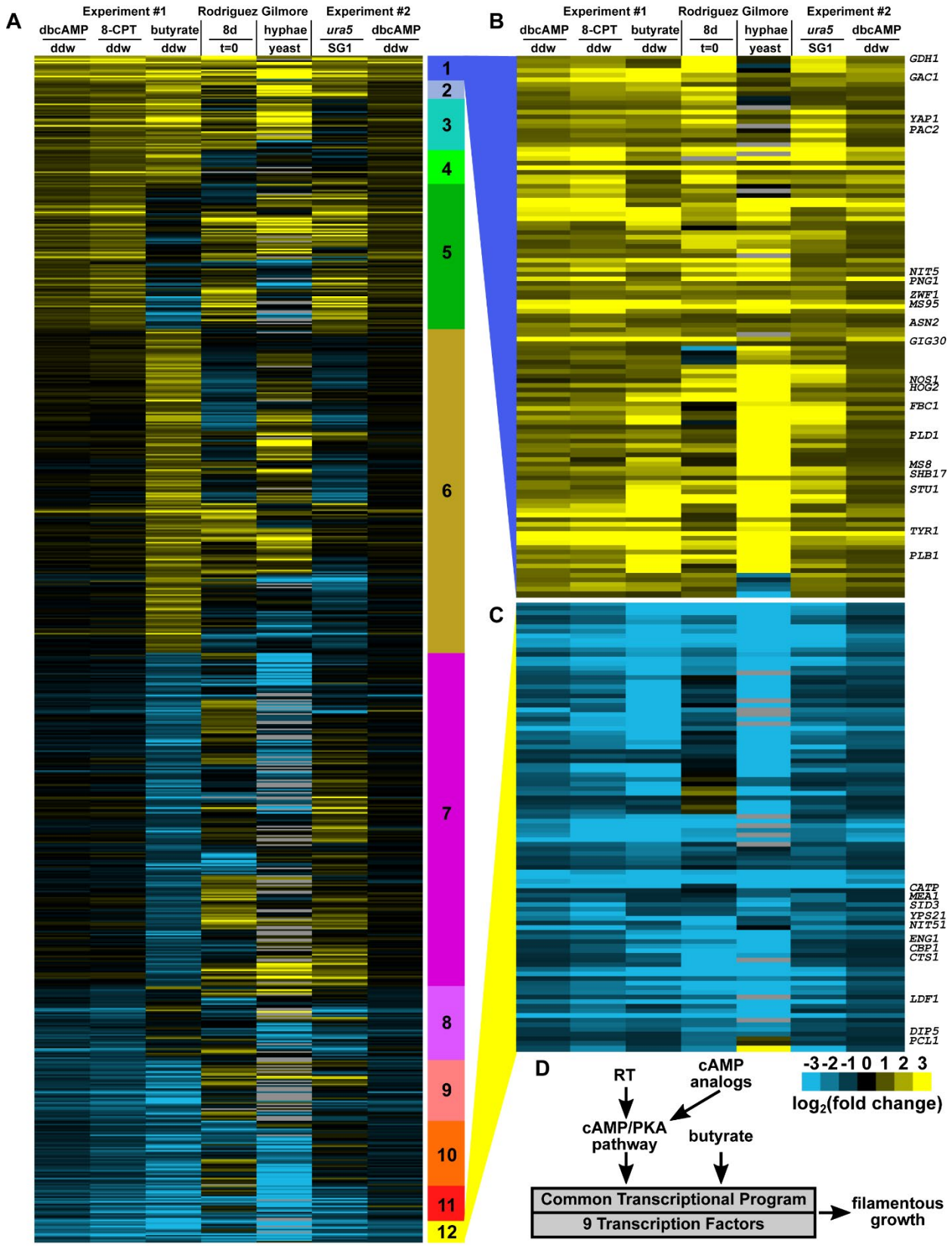
A
Experiment #1
Rodriguez Gilmore
Experiment #2
dbcAMP
8-CPT
butyrate
8d
hyphae
ura5
dbcAMP
ddw
ddw
ddw
t=0
yeast
SG1
ddw
1
2
3
4
5
6
7
8
9
10
11
12
B
C
GDH1
GAC1
YAP1
PAC2
NIT5
PNG1
ZWF1
MS95
ASN2
GIG30
NQS1
HOG2
FBC1
PLD1
MS8
SHB17
STU1
TYR1
PLB1
CATP
MEA1
SID3
YPS21
NIT51
ENG1
CBP1
CTS1
LDF1
DIP5
PCL1
D
RT
cAMP analogs
cAMP/PKA pathway
butyrate
Common Transcriptional Program
9 Transcription Factors
filamentous growth
-3 -2 -1 0 1 2 3
log2(fold change)

Figure 2.5. Genetic and environmental perturbations define high confidence morphology regulons.
(A) Heatmap showing 5494 genes differentially expressed in response to butyrate, dbcAMP, or 8-CPT-cAMP. Genes are grouped by expression pattern according to the scheme in **Fig. 2.4** as indicated by the colored bar to the right of the heatmap. Heatmap colors indicate $\log_2$ ratios of cpm values. (B) Expanded view of the high confidence yeast regulon (class 1, 112 genes). (C) Expanded view of the high confidence hyphal regulon (class 12, 93 genes). (D) Summary of experiments and analysis used to identify 9 TFs that increase in abundance under multiple filamentation conditions.

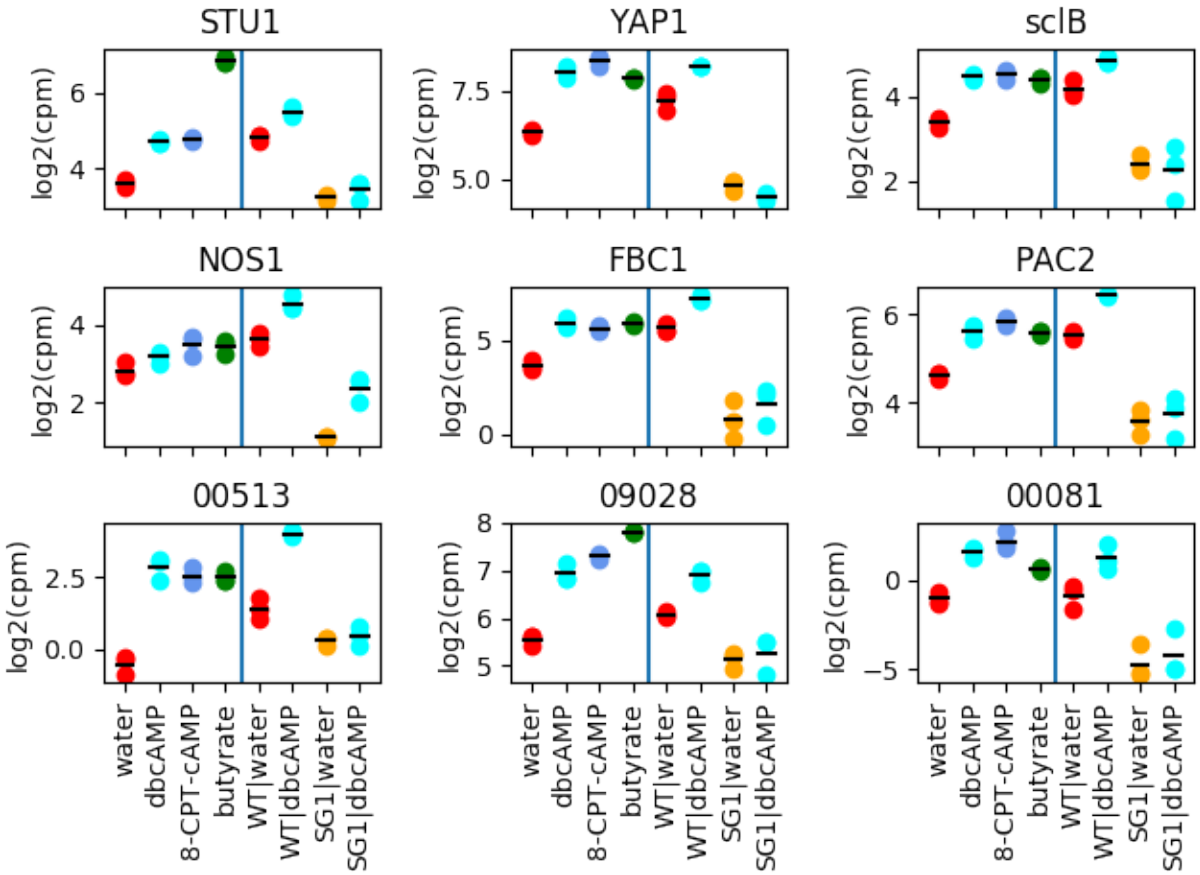

Figure 2.6. The stringent filamentous transcript set contains 9 transcription factors.
Transcript abundances of transcription factors in the stringently filamentous gene group (class 1 in **Figure 2.5A, B**), reported as $\log_2$ of read counts per million (cpm) in two separate experiments (as indicated by the two halves of each box). The conditions for the left half of each box are water, dbcAMP, 8-CPT-cAMP and butyrate for the wild-type strain. Conditions for the right half of each box are either water or dbcAMP for either the wild-type or SG1 strain, as indicated. Short black lines represent LIMMA fit values of transcript abundances for each condition. Each box is labeled with the name of the corresponding TF or a ucsf_hc.01_1.G217B transcript number for unannotated TFs (S5 Data of (Gilmore et al., 2015)).

The WOPR TF *PAC2* and the C2H2 TF *FBC1* are necessary for cAMP-induced filamentation

Our transcriptional analysis indicated that 9 TFs change in expression in our dataset of interest (**Fig. 2.6 and 2.5D**). We chose to focus on three of these TFs, all of which have orthologs that affect morphology and basic biology of other fungi. We chose the APSES TF *STU1*, which has previously been shown to affect aerial hyphae formation in *Histoplasma* (Longo et al., 2018) and whose ectopic expression stimulates inappropriate filamentation at 37°C (Rodriguez et al., 2019). *STU1* is homologous to the *Candida albicans* TF *EFG1*. In *C. albicans*, cAMP production in response to diverse filamentation cues has been shown to activate protein kinase A, in turn activating Efg1 to promote filamentous growth and repress the transcriptional program governed by TFs such as the WOPR TF White-opaque regulator 1 (Wor1) (Bockmühl and Ernst, 2001). In addition, we subjected the WOPR TF *PAC2*, whose ortholog in *Schizosaccharomyces pombe* has a role in repression of mating (Kunitomo et al., 1995), to further study. We also examined the role of *FBC1*, a C2H2 transcription factor orthologous to *Aspergillus* spp. FlbC, which is necessary for appropriate conidiation (Kwon et al., 2010).

To test whether *STU1*, *FBC1*, or *PAC2* are necessary for filamentation in response to exogenous cAMP or in response to room temperature, we used CRISPR/Cas9 technology (Nødvig et al., 2015; Kujoth et al., 2018) to delete the open reading frame of these genes, or to disrupt them by introducing an indel, causing a frame shift and premature termination (Fig. 4A). The *stu1* mutant exhibited filamentous growth in response to dbcAMP or to room temperature, much like the parental wild-type strain (**Fig. 2.7B** and **2.7C**), indicating that *STU1* is not necessary for dbcAMP- or room temperature-induced filamentation in liquid media. In contrast, neither the *pac2* nor the *fbc1* mutant produced hyphae when exposed to dbcAMP, indicating that dbcAMP-induced filamentation is dependent on each of these TFs. Interestingly, both mutants were able to transition to hyphal growth within 8 days of room temperature growth,

although under these conditions there is less filamentation in the *fbc1* mutant strain (**Fig. 2.7C**). Nonetheless, *PAC2* and *FBC1* are individually dispensable for room temperature-induced filamentation.

Since fungi exhibit morphologic changes on solid medium, we examined the phenotype of G217B*ura5* (parental strain), *stu1*, *pac2*, and *fbc1* strains on solid Sabouraud media at room temperature. We observed that the parental strain generated large amounts of macroconidia (**Fig. 2.7D**). In contrast, the *stu1*, *pac2*, and *fbc1* mutants were each deficient in the formation of these cells (**Fig. 2.7D**). Additionally, when grown on HMM plates containing GlcNAc at room temperature, these mutants yielded glossy, pink colonies as opposed to the fuzzy orange-brown colonies of the parental G217B*ura5* (**Fig. 2.7E**), although both colonies consisted of filamentous cells (data not shown). Taken together, these data indicate that each of these transcription factors is required for the normal developmental program, including macroconidia formation and pigment production, on solid medium at room temperature.

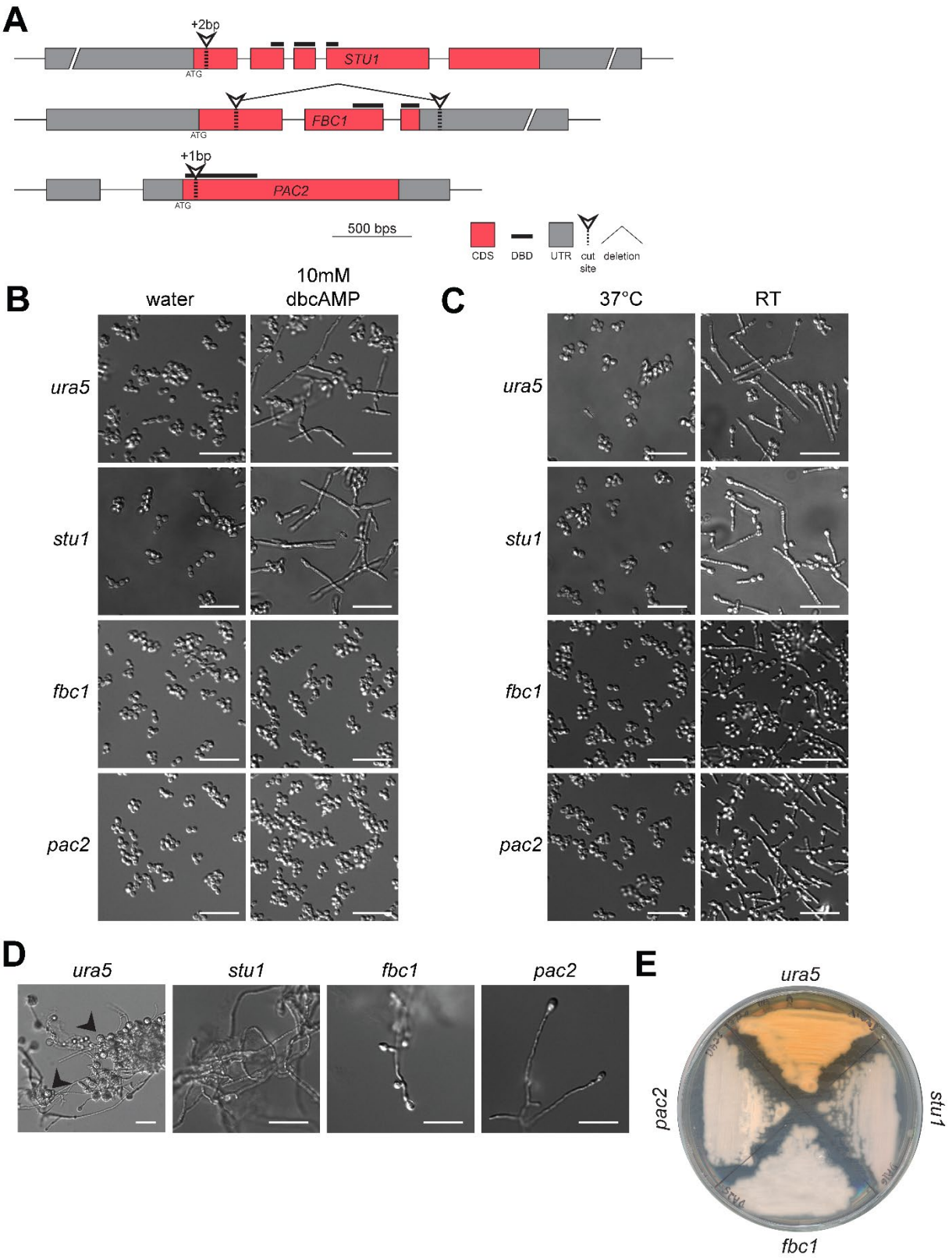
A
+2bp
STU1
ATG
FBC1
ATG
+1bp
PAC2
ATG
500 bps
CDS
DBD
UTR
cut site
deletion
B
water
10mM dbcAMP
ura5
stu1
fbc1
pac2
C
37°C
RT
ura5
stu1
fbc1
pac2
D
ura5
stu1
fbc1
pac2
E
ura5
stu1
fbc1
pac2

Figure 2.7. Transcription factors *PAC2* and *FBC1* are necessary for cAMP-induced filamentation.
(A) Scheme summarizing genetic manipulations of *Histoplasma* using CRISPR/Cas9 to disrupt *STU1* and *PAC2*, and delete the open reading frame of *FBC1*. (B) Cell morphology of G217B*ura5* (parental strain), *stu1*, *pac2*, and *fbc1 Histoplasma* after 2 days of growth at 37°C in liquid HMM containing GlcNAc with or without 10mM dbcAMP. (C) Cell morphology of G217B*ura5* (parental strain), *stu1*, *pac2*, and *fbc1 Histoplasma* after 8 days of growth at RT in liquid HMM containing GlcNAc. (D) Cell morphology of G217B*ura5* (parental strain), *stu1*, *pac2*, and *fbc1 Histoplasma* after 8 days of growth at RT on solid Sabouraud media. Arrows indicate macroconidia. (E) Gross growth morphology of G217B*ura5* (parental strain), *stu1*, *pac2*, and *fbc1 Histoplasma* after 14 days of growth at RT on solid HMM+GlcNAc media. bp: base-pair; CDS: coding sequence; DBD: DNA binding domain; UTR: untranslated region; scale bar denotes 10 µm.

Ectopic expression of *PAC2* and *FBC1* stimulates inappropriate filamentation at 37°C

Ectopic expression of *STU1* is sufficient to override the yeast program and promote robust filamentation at 37°C (Rodriguez et al., 2019). To test whether deregulated expression of *PAC2* and *FBC1* has a similar phenotype at 37°C, we used a constitutive *ACT1* promoter to drive their expression. Ectopic expression of *PAC2* resulted in filamentous colonies at 37°C, while ectopic expression of *FBC1* resulted in an aberrant wrinkled colony at 37°C containing both yeast and hyphae (**Fig. 2.8A**). To understand the relationships between the activity of the three transcription factors, we also ectopically expressed each one of them in the background of the three mutants. Overexpression of *FBC1* in the *stu1* mutant did not result in filamentation at 37°C, and overexpression of *PAC2* in the *stu1* mutant resulted in a mixed yeast-hyphae morphology. In contrast, ectopic expression of *STU1* triggered filamentation at 37°C in both the *fbc1* and *pac2* mutants, suggesting that Stu1 functions downstream of Fbc1 and Pac2. In contrast, ectopic expression of *FBC1* had a much less dramatic phenotype in the *pac2* mutant compared to the parental strain, indicating that the effect of *FBC1* overexpression is dependent on *PAC2*. Conversely, ectopic expression of *PAC2* was able to promote filamentous growth at 37°C in both the *fbc1* and *pac2* mutants (**Fig. 2.8A**). Taken together, these results show that the

ability of Fbc1 to induce filamentous growth at 37°C depends on the activity of Pac2 and Stu1, and similarly Fbc1- and Pac2-dependent filamentation at 37°C depends on Stu1 (**Fig. 2.8B**).

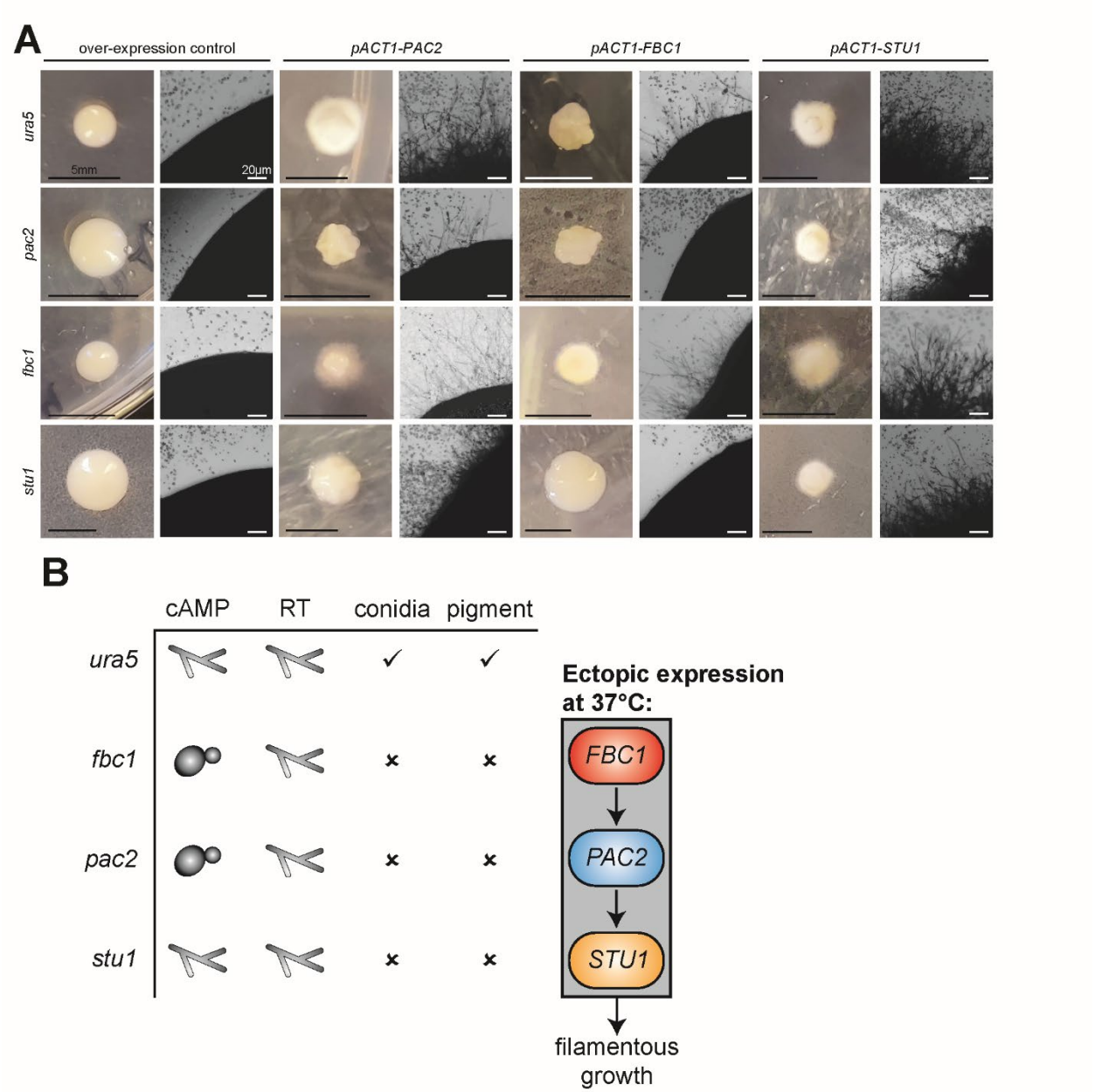

Figure 2.8. Expression of *PAC2* and *FBC1* is sufficient to trigger inappropriate filamentation at 37°C.
(A) Various *Histoplasma* strains (genotype indicated on the left) were transformed with ectopic expression constructs carrying *PAC2*, *FBC1*, or *STU1* (indicated on the top). For each transformation, a macroscopic image of colonies on the transformation plate is shown on the left, and a microscopic image of the corresponding colony edge is shown on the right. Untransformed microcolonies can be seen as small dark dots in the background of the microscopic images. (B) Table summarizing the *fbc1*, *pac2*, and *stu1* phenotypes and a model showing the genetic relationship between *FBC1*, *PAC2*, and *STU1* in the context of ectopic expression at 37°C.

Chapter 3 – Discussion

In this study we have shown that exogenous cAMP is sufficient to promote filamentous growth in *Histoplasma* by triggering transcriptional reprogramming at 37°C. We compared the transcriptional response to three filamentation signals—the classic physiological signal of RT, exogenous cAMP at 37°C, and exogenous butyrate at 37°C. We determined that 9 transcription factors are induced by all three of these signals and hypothesized that these factors regulate the hyphal growth program. We focused on three such factors that were induced by cAMP and repressed in the non-filamenting mutant SG1: *STU1*, *FBC1*, and *PAC2*. We have shown that while *STU1* is dispensable for cAMP-induced filamentation, *PAC2* and *FBC1* each are necessary for cAMP-induced filamentation. Each of these transcription factors is not individually necessary for room temperature-induced filamentation in liquid media, although each transcription factor is necessary for normal hyphal development (including macroconidia and pigment production) on solid media. Finally, we have shown that ectopic expression of *STU1*, *FBC1*, or *PAC2* is sufficient to drive filamentous growth at 37°C, that the ability of *FBC1* to promote filamentous growth at 37°C is dependent on *PAC2*, and that the ability of *FBC1* and *PAC2* to promote filamentous growth depends on *STU1*, suggesting the transcription factor hierarchy depicted in Figure 5B.

We utilized two chemical stimuli that promote filamentation despite growth at 37°C: cyclic AMP and butyrate. While the ability of exogenous cAMP to promote filamentation in *Histoplasma* has been described in the literature (Sacco et al., 1981), the transcriptional changes that occur during cAMP treatment were unknown. Additionally, this study is the first to observe the ability of butyrate to promote filamentous growth. We initially investigated butyrate to determine if its release from dibutyryl-cAMP, a cAMP analog commonly used to study PKA activation, was responsible for the response of *Histoplasma* to dbcAMP. However, the response of *Histoplasma* to butyrate is distinct from its response to dbcAMP: Butyrate is a much more

potent filamentation stimulus, it triggers a unique transcriptional response, and the transcriptional response of *Histoplasma* to dbcAMP is near-identical to its transcriptional response to 8-CPT-cAMP, which does not contain butyrate. Thus, we conclude that the effects of dbcAMP are not due to release of butyrate from this compound but rather via its activity in the cAMP pathway.

To identify gene sets that correspond with the morphological transition to filamentous growth, we conducted expression profiling of cultures filamenting in response to dbcAMP and to butyrate. About 46% of the total transcriptome is differentially expressed in samples treated with butyrate. Specifically, we detected up-regulation of lipid metabolic genes, ergosterol synthesis genes, and ribosomal proteins in response to butyrate. While the up-regulation of ribosomal proteins may be connected with the change in the proteome that is necessary to establish a different growth form (yeast *vs.* filaments), the role of lipid metabolism genes in this context remains to be elucidated.

It is unclear whether the transcriptional response to butyrate reflects a physiologically relevant response to butyrate as a filamentation-inducing signal; e.g., *Histoplasma* may naturally encounter soil-residing bacteria, which are capable of producing butyrate (Buckel, 2001). Interestingly, butyrate can act as a pan-histone deacetylase inhibitor (HDACi) (Davie, 2003). In other fungi, HDACi (including butyrate) have been shown to affect developmental programs: a study conducted in *C. albicans*, *C. parapsilosis*, and *C. neoformans* found that butyrate decreased fungal growth and biofilm formation in *Candida albicans* and *C. parapsilosis*, inhibited filamentation in *C. albicans*, and prevented capsule formation and melanization in *C. neoformans* (Nguyen et al., 2011). Introduction of butyrate or other HDACi, as well as genetic disruption of HDACs, has also been shown to modulate diverse processes such as virulence, morphology, conidiation, germination, and the expression of secondary metabolite (SM) gene clusters in *Aspergillus*, *Magnaporthe*, *Cryptococcus*, *Cochiobolus carbonum*, and others (Zutz et

al., 2013; Shwab et al., 2007; Izawa et al., 2009; Pidroni et al., 2018; Brandão et al., 2015; Broschla et al., 1995).

In contrast to butyrate, the cAMP analogs dbcAMP and 8-CPT-cAMP only affected the expression of 25% of the transcriptome. We did not detect any concerted regulation of carbon utilization pathways in our data in response to cAMP. However, 15 genes involved in amino acid synthesis pathways are upregulated in response to dbcAMP, as well as both subunits of the fatty acid synthase (FAS) complex, suggesting that, similar to *S. cerevisiae* (Broach, 2012; Thevelein and de Winde, 1999; Conrad et al., 2014), *Histoplasma* up-regulates biosynthetic pathways in response to cAMP. Interestingly, the OLE1 Δ9-desaturase, which Storlazzi *et al*. have previously reported to be down-regulated in response to exogenous cAMP (Storlazzi et al., 1999), is up-regulated in response to cAMP in our experiments. *OLE1* is not differentially expressed in the steady-state yeast or mycelial phases of *Histoplasma* G217B (Gilmore et al., 2015), but appears to be consistently upregulated in the days following the transition of *Histoplasma* cultures to room temperature (Rodriguez et al., 2019). These data are contrary to the finding reported by Gargano *et al.* (Gargano et al., 1995) that *OLE1* transcript was present in G217B yeast but absent in mycelia. Future experiments to target *OLE1* levels could address the function of this gene in morphogenesis. For example, increase of Ole1 activity could lead to elevated levels of unsaturated fatty acids in cellular membranes, with potential consequences on signaling cascades, thermotolerance and virulence.

By comparing differential expression induced by both cAMP analogs and butyrate with existing data for differential expression between 37°C and RT and between WT *Histoplasma* and the non-filamenting SG1 mutant, we arrived at high-confidence filamentation- and yeast-associated gene groups. By definition, these groups are well-correlated with previously defined morphology-associated groups that compared gene expression in response to room temperature with that of SG1 (Rodriguez et al., 2019). The stringent yeast group is enriched for Ryp1, Ryp2 and Ryp3 direct targets, and contains several genes encoding small, secreted

proteins and genes involved in iron acquisition, all hallmarks of the *Histoplasma* yeast phase. Interestingly, this group is largely devoid of genes encoding known regulators and transcription factors. An exception is Mea1, the ortholog of the *A. nidulans* nitrogen regulator MeaB, which is involved in the regulation of nitrogen metabolism (Polley and Caddick, 1996).

In contrast, the stringent gene group associated with filamentous growth contains multiple transcripts encoding signaling molecules and transcription factors, as well as transcripts that suggest an upregulation of the pentose phosphate pathway (*ZWF1*, *SHB17*), lipid biosynthesis (*FAS1*, *FAS2*, *GIG30*), and lipid processing (phospholipases B and D). A connection between cell morphology and the metabolic state of *Histoplasma* remains to be elucidated in future studies.

The stringent hyphal-associated gene group contains 9 genes predicted to function as transcription factors, of which 6 have previously been associated with regulation of morphology and development in other fungi: the Znc1 ortholog in *Y. lipolytica* regulates filamentation (Martinez-Vazquez et al., 2013); sclB regulates conidiation and SM production in *A. nidulans* (Thieme et al., 2018); *STU1* encodes an APSES transcription factor, and its orthologs stuA and Efg1 regulate development and morphology in *Aspergillus* and *Candida*, respectively (Miller et al., 1992; Stoldt et al., 1997; Glazier, 2022); Fbc1 ortholog flbC regulates conidiation in *Aspergillus* (Kwon et al., 2010); NosA regulates sexual development in *A. nidulans* (Vienken and Fischer, 2006b); and *PAC2* encodes a WOPR family transcription factor, orthologous to S. pombe *pac-2*, which represses the cAMP-dependent expression of *ste-11*, thus inhibiting mating (Kunitomo et al., 1995). Together, this group of transcription factors are attractive candidates for regulators that are relevant to the ability of *Histoplasma* to switch between the yeast and hyphal morphology.

We chose to further characterize the role of three of these transcription factors in promoting filamentation in response to cAMP and RT: *PAC2*, *FBC1*, and *STU1*. While *PAC2* and *FBC1* were necessary to trigger filamentous growth in response to cAMP, *STU1* was

dispensable for cAMP-dependent filamentation, and none of these three transcription factors were necessary for RT-induced filamentation in liquid culture. Although we reported previously that disruption in the promoter region of *STU1* has a partial filamentation phenotype, we did not observe the same phenotype in liquid culture in the ORF-disruption mutant we generated in this study. However, we did observe a RT phenotype on plates. In fact, mutants lacking functional Pac2, Fbc1, or Stu1 each had developmental defects in the full hyphal program at RT (**Fig. 2.7D, E)**. Additionally, we found that overexpression of each of the transcription factors was sufficient to drive filamentous growth at 37°C (**Fig. 2.8A**). Additional work is needed to determine whether these, and other transcription factors whose expression is correlated with filamentous growth, act redundantly to drive filamentation in liquid culture in response to temperature.

Our ectopic expression work uncovered interesting relationships between Pac2, Fbc1, and Stu1. We found that *PAC2* was necessary for *FBC1*-driven filamentation, and similarly, *STU1* was necessary for *FBC1* and *PAC2* ectopic expression to cause filamentous growth at 37°C. Together, this suggests a genetic pathway with *PAC2* downstream of *FBC1*, and *STU1* downstream of *PAC2* (**Fig. 2.8B**). However, regulation of eukaryotic transcription is often complex, and further research is necessary to determine the roles of these 3 transcription factors in controlling and coordinating the transcriptional response to cAMP. We note that *PAC2*, which we have implicated in the hyphal program in this study, and *RYP1*, which is required for the yeast program, are paralogs, suggesting specialization of these individual TFs in opposing developmental programs. Further exploring the circuits that govern the transition between yeast and hyphae in thermally dimorphic fungi will elucidate the critical basic biology of these pathogens and provide an opportunity to develop molecular strategies for targeted therapeutics.

Open Questions

Is cAMP necessary for the yeast-to-hyphae transition?

I have shown that increasing cAMP levels, either due to inhibition of phosphodiesterase or by addition of cAMP analogs, is sufficient to produce hyphal growth in *Histoplasma*. While there is a correlation between cAMP levels and filamentation, it remains unknown whether an increase in cAMP is strictly necessary for the normal yeast-to-hyphae transition induced by growth at RT. Thus far, attempts to chemically inhibit adenylate cyclase, or to disrupt it genetically were not successful (data not shown), possibly because its function may also be essential for growth in the yeast phase; however, other approaches, such as RNA interference, may be suitable to answer this question.

How is the cAMP-PKA pathway in *Histoplasma* triggered, and what are its direct targets?

As detailed in the introduction, extensive research has been done to identify the components of the cAMP-PKA pathway in *S. cerevisiae*, *C. albicans*, *Aspergilli* and a handful of other fungi, while much less is known about the specific mechanisms of this pathway in other fungi, and particularly thermally dimorphic fungi. A better understanding of the events that trigger cAMP production and PKA activation in *Histoplasma*, and what are the phosphorylation targets of PKA will further our understanding of how temperature signals translate into molecular events that control cellular morphology.

Are there transcriptional regulators that are necessary for filamentation?

In this study, we have identified 9 putative transcriptional regulators whose transcripts' abundances rise in response to cAMP, butyrate, and RT, and fail to do so in a mutant that does not filament in response to cAMP. We have also shown that expression of 3 of those genes, *STU1*, *FBC1*, and *PAC2*, is sufficient to trigger filamentous growth at 37°C. However, genetically disrupting any of those genes does not cause a defect in the RT-induced transition from yeast to

hyphal growth. It would be interesting to examine the role of the remaining transcriptional regulators and potentially identify a transcriptional regulator that is necessary for hyphal growth. Alternatively, there is a possibility that these regulators act redundantly, and thus multiple factors need to be disrupted in order to have an effect on RT-induced filamentation.

What is the regulon controlled by *STU1*, *FBC1*, and *PAC2*?

Ectopic expression of either *STU1*, *FBC1*, or *PAC2* causes filamentous growth at 37°C, while their disruption causes aberration in normal development at RT, such as a defect in conidiation and decrease in pigmentation on solid media containing GlcNAc. More in depth analysis of how these transcriptional regulators affect the transcriptional program in different growth conditions would allow us to better understand the genetic circuits that govern morphology in *Histoplasma*.

Materials and Methods

H. capsulatum strains and growth conditions

All strain manipulations were done in G217B*ura5*-DA, which is derived from the *Histoplasma* G217B*ura5* (WU15) background. Strains used in this paper can be found in **Table 1**. Strain frozen stocks (8% DMSO or 15% Glycerol) were streaked onto *Histoplasma* Macrophage Medium (HMM) agarose plates supplemented with 0.2mg/ml uracil where necessary. Liquid *Histoplasma* cultures were inoculated from solid media plates into HMM + 100 U/ml Penicillin/ Streptomycin (with 0.2mg/ml of uracil if needed) and were passaged 1:25 every 2-3 days into fresh medium, unless indicated otherwise. The glucose in HMM was replaced with equimolar amounts of N-acetyl-glucosamine (A3286, Sigma Aldrich) in indicated experiments. Where mentioned, dibutyryl cyclic adenosine monophosphate sodium (dbcAMP, D0627, Sigma Aldrich), 8-(4-Chlorophenylthio)-cAMP sodium (8-CPT-cAMP, ab120424, Abcam), 3-isobutyl-1-methylxanthine (IBMX, ab120840, Abcam), sodium butyrate (B5887, Sigma Aldrich), or cyclic adenosine monophosphate sodium (cAMP, A6885, Sigma Aldrich) were added to cultures after dissolving in autoclaved water and filter sterilizing by passing through a 0.22 MCE filter (Santa Cruz Biotechnologies). For 37°C growth, plates were grown in a humidified incubator with 5% CO_2, and liquid cultures were grown on an orbital shaker at 120-150rpm. For room temperature (RT) growth, plates were wrapped in parafilm and plastic bags and placed in a 25°C incubator in a Biosafety level 3 facility. Liquid RT cultures were grown at ambient temperature (26-28°C) on an orbital shaker at 120 rpm.

Strains and Cloning

The SG1 mutant was generated using *Agrobacterium*-mediated insertional mutagenesis as described previously (Rodriguez et al., 2019). Subcloning was performed in *E. coli* DH5α- or DH10b-derived strains. The *STU1* overexpression strain and the control strain were constructed

as described previously (Rodriguez et al., 2019). *FBC1* and *PAC2* overexpression strains were constructed by amplifying the open reading frame (ORF) and 3' untranslated region (3'UTR) by PCR, and cloned into pTM1 (a pDONR/Zeo based plasmid) downstream of the ACT1 promoter using Gibson cloning kit (NEB), and then introduced into pDG33 using Gateway cloning (Thermo Fisher Scientific). To introduce gene disruption, we used the strategy described previously (28, 29, Joehnk et al, in preparation). Briefly, a gene-appropriate protospacer was inserted into a self-cleaving element using PCR and cloned into the episomal plasmid pBJ219 (which contains the *HcURA5* gene) using Gateway cloning. The plasmid was linearized and introduced into *Histoplasma* G217B*ura5* using electroporation (as described previously in (Hwang et al., 2008)) along with an mCherry-targeting protospacer as a negative control. Transformants that grew on HMM without uracil were assayed for the disruption using PCR amplifying the targeted genomic region followed by sequencing of the product and indel analysis using the ICE tool (inference of CRISPR edits) from Synthego. The colony with the highest indel levels was selected, grown on fresh media, and plated for single colonies. The process was repeated until no wild-type sequence could be detected. The plasmid was then lost by growing the isolate for 3 passages in liquid media containing uracil, plating the culture for single colonies and identifying colonies that were auxotrophic for uracil. To create whole gene deletion mutants, the aforementioned technique was adapted to include two protospacers targeting the sequences 5' and 3' of the gene. To test for a deletion, DNA was extracted from a liquid *Histoplasma* culture, and PCR with primers external to the deleted sequence, or with primers internal to the sequence, was performed. The colony with highest amount of editing (short external PCR product, lowest levels of internal PCR product) were selected, grown on fresh media, and plated for single colonies. The process was repeated until no wild-type sequence could be detected.

Table 4.1: Strains used in this study

Name	Referred in this study as	Comment
G217B-DA	G217B	Derived from ATCC 26032 through passaging.
G217B*ura5*-DA	G217B*ura5* or *ura5*	Derived from WU15 through passaging; Parental strain used to generate CRISPR mutants.
G217B*ura5 msb2*::T-DNA	SG1	WU15 with T-DNA insertion upstream of *MSB2* ORF (Rodriguez et al., 2019).
G217B*ura5*-DA *fbc1*Δ	*fbc1*	Deletion strain of *FBC1* (ATG+273..1555 deleted).
G217B*ura5*-DA *pac2-1*	*pac2*	Disruption strain of *PAC2* (1 bp insertion in position ATG+33).
G217B*ura5*-DA *stu1-2*	*stu1*	Disruption strain of *STU1* (2 bp insertion in position ATG+26).
G217B*ura5*-DA p*ACT1*-t*CATB*; *URA5*	*ura5* + Overexpression control	Overexpression control.
G217B*ura5*-DA p*ACT1-FBC1*-t*CATB*; *URA5*	*ura5* + *pACT1-FBC1*	Overexpression of *FBC1*.
G217B*ura5*-DA p*ACT1-PAC2*-t*CATB*; *URA5*	*ura5* + *pACT1-PAC2*	Overexpression of *PAC2*.
G217B*ura5-DA* p*ACT1-STU1*-t*CATB*; *URA5*	*ura5* + *pACT1-STU1*	Overexpression of *STU1*.
G217B*ura5*-DA *fbc1*Δ p*ACT1*-t*CATB*; *URA5*	*fbc1* + Overexpression control	Overexpression control in the *fbc1* strain.
G217B*ura5*-DA *fbc1*Δ p*ACT1-FBC1*-t*CATB*; *URA5*	*fbc1* + *pACT1-FBC1*	Overexpression of *FBC1* in the *fbc1* strain.
G217B*ura5*-DA *fbc1*Δ p*ACT1-PAC2*-t*CATB*; *URA5*	*fbc1* + *pACT1-PAC2*	Overexpression of *PAC2* in the *fbc1* strain.
G217B*ura5*-DA *fbc1*Δ p*ACT1-STU1*-t*CATB*; *URA5*	*fbc1* + *pACT1-STU1*	Overexpression of *STU1* in the *fbc1* strain.
G217B*ura5*-DA *pac2-1* p*ACT1*-t*CATB*; *URA5*	*pac2* + Overexpression control	Overexpression control in the *pac2* strain.
G217B*ura5*-DA *pac2-1* p*ACT1-FBC1*-t*CATB*; *URA5*	*pac2* + *pACT1-PAC2*	Overexpression of *FBC1* in the *pac2* strain.
G217B*ura5*-DA *pac2-1* p*ACT1-PAC2*-t*CATB*; *URA5*	*pac2* + *pACT1-PAC2*	Overexpression of *PAC2* in the *pac2* strain.
G217B*ura5*-DA *pac2-1* p*ACT1-STU1*-t*CATB*; *URA5*	*pac2* + *pACT1-STU1*	Overexpression of *STU1* in the *pac2* strain.
G217B*ura5*-DA *stu1-2* p*ACT1*-t*CATB*; *URA5*	*stu1* + Overexpression control	Overexpression control in the *stu1* strain.
G217B*ura5*-DA *stu1-2* p*ACT1-*	*stu1* + *pACT1-FBC1*	Overexpression of *FBC1*

Name	Referred in this study as	Comment
FBC1*-t*CATB*; *URA5		in the *stu1* strain.
G217B*ura5*-DA *stu1-2* p*ACT1-PAC2*-t*CATB*; *URA5*	*stu1* + *pACT1-PAC2*	Overexpression of *PAC2* in the *stu1* strain.
G217B*ura5*-DA *stu1-2* p*ACT1-STU1*-t*CATB*; *URA5*	*stu1* + *pACT1-STU1*	Overexpression of *STU1* in the *stu1* strain.

Table 4.2: Primers used in this study

Number	Sequence	Purpose	Template
Primers for cloning of the STU1 CRISPR/Cas9 plasmid			
5699	ATGGCAGAGCTCCAGTCATC	Amplify the 5' segment of gRNA cassette.	pPTS608-Cas9-hyg-Pra1-sgRNA (Kujoth et al., 2018)
7351	GACGAGCTTACTCGTTTCGTCCTCACGGACTCATCAGAATGTGCGGTGATGTCTGCTCAAGC	Amplify the 5' segment of gRNA cassette. Underlined: gene specific sequence.	pPTS608-Cas9-hyg-Pra1-sgRNA
5702	TTTGCTTTTCCCGAACTT	Amplify the 3' segment of gRNA cassette.	pPTS608-Cas9-hyg-Pra1-sgRNA
7350	GGACGAAACGAGTAAGCTCGTCAATGTGATGCATGTACATCCGTTTTAGAGCTAGAAATAGCAAG	Amplify the 3' segment of gRNA cassette. Underlined: gene specific sequence.	pPTS608-Cas9-hyg-Pra1-sgRNA
5769	GGGGACAAGTTTGTACAAAAAAGCAGGCTGCGTAAGCTCCCTAATTGGC	Fusing the 5' and 3' segments and adding attB sites.	5' + 3' segments
5770	GGGGACCACTTTGTACAAGAAAGCTGGGTGAGCCAAGAGCGGATTCCT	Fusing the 5' and 3' segments and adding attB sites.	5' + 3' segments
Primers for amplification and testing the efficiency of the CRISPR/Cas9 disruption of STU1			
6326	CCGTGCCCAGTTATACGACG	To sequence the *STU1* disruption site.	G217B *STU1* locus
3109	GCACAGCAATCCTCCTCTTC	To amplify *STU1* around disruption site.	G217B *STU1* locus
6327	CATCGGCCCTATTTTGACGACAT	To amplify *STU1* around disruption site.	G217B *STU1* locus
Primers for cloning of the FBC1 CRISPR/Cas9 plasmid			
6631	*GCCCGGGC*TAACTTGTTGCGTTCC	Amplify the 5' segment of gRNA cassette. Italicized: SrfI site.	pPTS608-Cas9-hyg-Pra1-sgRNA
7369	GACGAGCTTACTCGTTTCGTCCTCACGGACTCATCAGCAGGGTCGGTGATGTCTGCTCAAGC	Amplify the 5' segment of gRNA cassette. Underlined: gene specific sequence.	pPTS608-Cas9-hyg-Pra1-sgRNA

Number	Sequence	Purpose	Template
7371	GACGAGCTTACTCGTTTCGTCCTCACGGACTCATCAGACCCCACGGTGATGTCTGCTCAAGC	Amplify the 5' segment of gRNA cassette. Underlined: gene specific sequence.	pPTS608-Cas9-hyg-Pra1-sgRNA
5708	GAGCCAAGAGCGGATTCCT	Amplify the 3' segment of gRNA cassette.	pPTS608-Cas9-hyg-Pra1-sgRNA
7368	GGACGAAACGAGTAAGCTCGTCCAGGGTTGTAATTACTGCTCGTTTTAGAGCTAGAAATAGCAAG	Amplify the 3' segment of gRNA cassette. Underlined: gene specific sequence.	pPTS608-Cas9-hyg-Pra1-sgRNA
7370	GGACGAAACGAGTAAGCTCGTCACCCCAACATGCTTACGGGGGTTTTAGAGCTAGAAATAGCAAG	Amplify the 3' segment of gRNA cassette. Underlined: gene specific sequence.	pPTS608-Cas9-hyg-Pra1-sgRNA
6630	GGGGACAAGTTTGTACAAAAAAGCAGGCT*GCCCGGGC*TAACTTGTTG	Fusing the 5' and 3' segments of gRNA cassette A and adding attB sites and SrfI site.	5' + 3' segments of cassette A
5770	GGGGACCACTTTGTACAAGAAAGCTGGGTGAGCCAAGAGCGGATTCCT	Fusing the 5' and 3' segments of gRNA cassette A and adding attB sites.	5' + 3' segments of cassette A
6329	CGCAACAAGTTAGCCCGAGCCAAGAGCGGATTCCT	Fusing the 5' and 3' segments of gRNA cassette B and adding a SrfI site.	5' + 3' segments of cassette B
6380	AAAAGCAGGCTGCCC*GCCCGGGC*TAACTTGTTG	Fusing the 5' and 3' segments of gRNA cassette B and adding a SrfI site.	5' + 3' segments of cassette B
Primers for amplification and testing the efficiency of the CRISPR/Cas9 deletion of FBC1			
7402	GCATCCCTCTTGTTTTCTTGTC	To amplify outside of the FBC1 deletion	G217B *FBC1* locus
7411	GAAGAAAAACTTATGAAGCCGTACCGTC	To amplify outside of the FBC1 deletion	G217B *FBC1* locus
7406	GACTACCTTTGATCAAGCCCAAG	To amplify a sequence inside of the FBC1 deletion	G217B *FBC1* locus
7408	TGGAGCTGTAGTCGGTGACG	To amplify a sequence inside of the FBC1 deletion.	G217B *FBC1* locus
Primers for cloning of the PAC2 CRISPR/Cas9 plasmid			
6631	*GCCCGGGC*TAACTTGTTGCGTTCC	Amplify the 5' segment of gRNA cassette. Italicized: SrfI site.	pPTS608-Cas9-hyg-Pra1-sgRNA

Number	Sequence	Purpose	Template
7373	GACGAGCTTACTCGTTTCGTCCTCACGGACTCATCAGCGGACACGGTGATGTCTGCTCAAGC	Amplify the 5' segment of gRNA cassette. Underlined: gene specific sequence.	pPTS608-Cas9-hyg-Pra1-sgRNA
5708	GAGCCAAGAGCGGATTCCT	Amplify the 3' segment of gRNA cassette	pPTS608-Cas9-hyg-Pra1-sgRNA
7372	GGACGAAACGAGTAAGCTCGTCCGGACACGTCCGCACACCCGGTTTTAGAGCTAGAAATAGCAAG	Amplify the 3' segment of gRNA cassette. Underlined: gene specific sequence.	pPTS608-Cas9-hyg-Pra1-sgRNA
6630	GGGGACAAGTTTGTACAAAAAAGCAGGCT*GCCCGGGC*TAACTTGTTG	Fusing the 5' and 3' segments of gRNA cassette and adding attB sites and SrfI site.	5' + 3' segments
5770	GGGGACCACTTTGTACAAGAAAGCTGGGTGAGCCAAGAGCGGATTCCT	Fusing the 5' and 3' segments of gRNA cassette and adding attB sites.	5' + 3' segments
Primers for amplification and testing the efficiency of the CRISPR/Cas9 disruption of PAC2			
7369	CCGTTATTGTATGACCAGGAG	To amplify *PAC2* around disruption site.	G217B *PAC2* locus
7399	TGTACAGATCTTTCGTACGG	To amplify *PAC2* around disruption site.	G217B *PAC2* locus
7397	tagGCTCCGGTTTTGTTTAGG	To sequence *PAC2* disruption site.	G217B *PAC2* locus
Cloning overexpression plasmids of FBC1 and PAC2			
7454	ACCTCGTTAAGTAGCCCACAATGACTATGGTTATCGAAAACCGAAACCG	To amplify the *FBC1* ORF and 3' UTR	G217B *FBC1* locus
7455	TATGGTATGAGGTTTGAGGCCGCGCACAGGTATTAATCAAGAG	To amplify the *FBC1* ORF and 3' UTR	G217B *FBC1* locus
7457	CTCGTTAAGTAGCCCACAATGGAGACGTATAACGGACACG	To amplify the *PAC2* ORF and 3' UTR	G217B *PAC2* locus
7456	CCTCAAACCTCATACCATATGCCCCGATTTGAGTCCTTTTCC	To amplify the *PAC2* ORF and 3' UTR	G217B *PAC2* locus
7420	TATGGTATGAGGTTTGAGGCGCAA	To linearize pTM1 (LR's) between the *ACT1* promoter and the *CATB* terminator	pTM1 (Rodriguez et al., 2019)
7421	TGTGGGCTACTTAACGAGGT	To linearize pTM1 (LR's) between the *ACT1* promoter and the *CATB* terminator	pTM1

Imaging and image analysis

DIC imaging was performed on a Zeiss AxioCam MRM microscope at 40× magnification. Colony images were captured using a Leica microscope. Gross morphology of colonies was captured using a OnePlus 8 Pro camera. To quantify filamentation events, Fiji was used to count yeast and filamentous events in 4 frames per sample.

Culture conditions for cAMP expression profiling experiments

Samples were prepared in two separate experiments. In the first experiment, *Histoplasma* G217B*ura5* was grown in liquid HMM culture at 37°C for 2 passages. On the day of chemical addition, the culture was passaged into fresh HMM + GlcNAc at a final OD600 of 0.2, and 10 mM dbcAMP, 4 mM 8-CPT-cAMP, 5 mM of sodium butyrate, or filter-sterilized autoclaved water (vehicle control) were added to the appropriate cultures, with 3 biological replicates for each chemical. Cultures were returned to 37°C growth with shaking. 2 days after the addition of each chemical, a small volume of each culture was fixed by adding paraformaldehyde (final paraformaldehyde concentration 4% v/v), and 10 ml of each culture were harvested by filtration using Nalgene Rapid-Flow Sterile Disposable Bottle Top Filters with SFCA Membrane (09-740-22G, Thermo Fisher Scientific). Cells were scraped from the filter into tubes and promptly flash-frozen in liquid nitrogen.

In the second experiment, *Histoplasma* G217B*ura5* or the SG1 mutant were grown in liquid HMM culture at 37°C for 2 passages. On the day of dbcAMP addition, the cultures were passaged into fresh HMM + GlcNAc at a final OD600 of 0.2, and 10 mM dbcAMP or filter-sterilized autoclaved water (vehicle control) were added to the appropriate cultures, with 3 biological replicates for each chemical-strain combination. The cultures were treated and samples were collected as described for the first experiment.

RNA extraction

Total RNA was extracted from fungal cells using a Qiazol-based RNA extraction protocol. Frozen cell pellets were resuspended in Qiazol (Qiagen) and incubated at RT for 5 minutes to thaw. The lysate was subjected to bead beating (Mini-Beadbeater, Biospec Products) followed by a chloroform extraction. The aqueous phase was then transferred to an Epoch RNA column where the filter was washed with 3 M NaOAc (pH=5.5) and then with 10 mM TrisCl (pH=7.5) in 80% EtOH. DNase (Purelink, Invitrogen) treatment was used to remove any residual DNA, and the filters were washed again with NaOAc and TrisCl before eluting the RNA in nuclease-free water.

mRNA isolation

For each experiment, mRNA was extracted from an equal amount of total RNA (up to 20 µg) of each sample. Total RNA samples and were treated with TURBO DNase (Thermo Fisher Scientific). RNA quality was determined with a RNA 6000 Nano Bioanalyzer chip (Agilent Technologies). mRNA was purified using polyA selection with Oligo-dT Dynabeads (Thermo Fisher Scientific) as described in the manufacturer's protocol. Ribosomal RNA depletion was confirmed with an RNA 6000 Nano Bioanalyzer chip.

RNAseq library preparation

Libraries for RNAseq were prepared using the NEB Next Ultra II Directional RNA Library Prep Kit (New England Biolabs). Individual libraries were uniquely barcoded with NEBNext Multiplex Oligos for Illumina sequencing platform (New England Biolabs). Average fragment size and presence of excess adapter was determined with High Sensitivity DNA Bioanalyzer chip from Agilent Technologies. Libraries had an average fragment length of 300 to 500 bp. The concentration of the individual libraries was quantified using the High Sensitivity DNA Qubit assay (Thermo Fisher Scientific). A total of 5 ng of each library was pooled into each final libraries and run on a High Sensitivity DNA Bioanalyzer chip to determine the average fragment

size of the final pooled samples. The final libraries were submitted to the UCSF Center for Advanced Technology for sequencing on an Illumina HiSeq 4000 sequencer.

Transcriptome analysis

Transcript abundances were quantified based on version ucsf_hc.01_1.G217B of the *Histoplasma* G217B transcriptome (S5 Data of (Gilmore et al., 2015)). Relative abundances (reported as TPM values (Li and Dewey, 2011)) and estimated counts (est_counts) of each transcript in each sample were estimated by alignment free comparison of k-mers between the reads and mRNA sequences using KALLISTO version 0.46.0 (Bray et al., 2016). Further analysis was restricted to transcripts with TPM ≥ 10 in at least one sample.
Differentially expressed genes were identified by comparing replicate means for contrasts of interest using LIMMA version 3.30.8 (Ritchie et al., 2015; Smyth, 2004). Genes were considered significantly differentially expressed if they were statistically significant (at 5% FDR) with an effect size of at least 1.5x (absolute log2 fold change ≥ 0.585) for a given contrast.
For comparison with previous expression profiling, the above KALLISTO/LIMMA pipeline was applied to the reads from (Gilmore et al., 2015) (SRA accession SRP058149) and LIMMA fit parameters were taken from S2 Data of (Rodriguez et al., 2019). Enrichments for Ryp1-3 targets in gene sets were calculated using a hypergeometric test, followed by Benjamini-Hochberg correction for multiple hypotheses testing, with adjusted $p < 0.05$ considered significant.

Protein extraction

Organic fractions from Qiazol-chloroform extraction were stored at –20°C. After thawing the fractions, 100% ethanol was added, and samples were centrifuged to pellet DNA. The protein-containing supernatant was added to isopropanol and centrifuged at 4°C to pellet the protein precipitate. The pellet was washed 3 times with 0.3M guanidinium thiocyanate in 95% ethanol followed by centrifugation at 4°C, after which 100% ethanol was added to the pellets.

The protein pellets were vortexed and incubated at RT for 20 minutes, centrifuged at 4°C, and air-dried at RT. The pellets were resuspended in urea lysis buffer (9 M Urea, 25 mM Tris-HCl, 1% SDS, 0.7 M β-mercaptoethanol) and incubated at 50°C up to 20 minutes until fully dissolved in the buffer, followed by boiling and centrifugation. The supernatant was transferred into a clean tube and quantified using the Pierce 660nm assay with added ionic detergent compatibility reagent (Thermo Fisher Scientific).

Western Blotting

Following quantification of protein, an equal amount per sample of 12 µg was boiled with Novex NuPAGE LDS Sample Buffer (Invitrogen) and loaded onto a Novex NuPAGE 4% to 12% BT SDS-PAGE gel (Invitrogen). Electrophoresis was performed in MOPS running buffer at 150 V. The protein was then transferred to a nitrocellulose membrane at approximately 35 V for 2 hours. The membrane was incubated with Intercept® (PBS) Blocking Buffer (LI-COR) for an hour and then incubated in the primary antibody in wash buffer overnight at 4 °C. Polyclonal peptide antibodies against either Ryp1, Ryp2, or Ryp3 were used as primary antibodies in the following dilutions in blocking buffer: rabbit anti-Ryp1 (1:10,000), rabbit anti-Ryp2 (1:2,500), rabbit anti-Ryp3 (1:5,000) (Beyhan et al., 2013). As a loading control, monoclonal mouse anti-α-tubulin (1:1,000) was used (DM1A, Novus Biologicals). The blot was washed with PBS + 0.1 % Tween-20 three times, and secondary antibody was added to the blot for 1 hour at room temperature: IRDye 800CW Goat anti-Rabbit IgG, or IRDye 680RD Donkey anti-Mouse IgG (both 1:10,000, LI-COR). The blot was washed with PBS + 0.1 % Tween-20 three times, and imaged using the LI-COR Odyssey CLx system.

***Histoplasma* genomic DNA extraction**

Cells from 10 mL of dense liquid culture were collected by centrifugation and kept at –80°C until DNA extraction. The cell pellets were thawed and washed in TE buffer, and then resuspended in lysis buffer (50 mM Tris [pH 7.2], 50 mM EDTA, 0.1 M SDS, 0.14 M β-

mercaptoethanol). Cells were lysed in buffer by bead-beating with zirconia beads, and the samples were incubated at 65°C for 1 hour. 800 µl of 1:1 phenol-chloroform solution was added to each sample followed by thorough mixing. The samples were centrifuged for 15 minutes at 13,000 rpm. The aqueous fraction was added to 470 µl of 0.13 M sodium acetate in 95 % isopropanol and mixed by inversion to precipitate the DNA. The supernatant was discarded after a 2-minute centrifugation, and the pellet was washed with 70% ethanol and air-dried at 65°C. 1 mL TE buffer with 1.5 µl RNase A (10mg/ml) was added to each sample and the pellet was dissolved at 65°C.

REFERENCES

Araúz, A.B., and Papineni, P., 2021. Histoplasmosis. *Infectious Disease Clinics of North America*, 35(2), pp.471–491.

Azimova, D., et al., 2022. Cbp1, a fungal virulence factor under positive selection, forms an effector complex that drives macrophage lysis. *PLoS pathogens*, 18(6), p.e1010417.

Bar-On, Y.M.,, Phillips, R., and Milo, R., 2018. The biomass distribution on Earth. *Proceedings of the National Academy of Sciences of the United States of America*, 115(25), pp.6506–6511.

Beyhan, S.,, Gutierrez, M.,, Voorhies, M., and Sil, A., 2013. A temperature-responsive network links cell shape and virulence traits in a primary fungal pathogen. *PLoS biology*, 11(7), p.e1001614.

Bockmühl, D.P., and Ernst, J.F., 2001. A potential phosphorylation site for an A-type kinase in the Efg1 regulator protein contributes to hyphal morphogenesis of Candida albicans. *Genetics*, 157(4), pp.1523–30.

Boy-Marcotte, E., et al., 1998. Msn2p and Msn4p control a large number of genes induced at the diauxic transition which are repressed by cyclic AMP in Saccharomyces cerevisiae. *Journal of Bacteriology*, 180(5), pp.1044–1052.

Brandão, F.A.S., et al., 2015. Histone deacetylases inhibitors effects on Cryptococcus neoformans major virulence phenotypes. *https://doi.org/10.1080/21505594.2015.1038014*, 6(6), pp.618–630.

Bray, N.L.,, Pimentel, H.,, Melsted, P., and Pachter, L., 2016. Near-optimal probabilistic RNA-seq quantification. *Nature biotechnology*, 34(5), pp.525–7.

Broach, J.R., 2012. Nutritional Control of Growth and Development in Yeast. *Genetics*, 192(1), pp.73–105.

Broschla, G., et al., 1995. Inhibition of maize histone deacetylases by HC toxin, the host-selective toxin of Cochliobolus carbonum. *The Plant Cell*, 7(11), pp.1941–1950.

Buckel, W., 2001. Unusual enzymes involved in five pathways of glutamate fermentation. *Applied Microbiology and Biotechnology 2001 57:3*, 57(3), pp.263–273.

Cao, C., et al., 2017. Global regulatory roles of the cAMP/PKA pathway revealed by phenotypic, transcriptomic and phosphoproteomic analyses in a null mutant of the PKA catalytic subunit in Candida albicans. *Molecular Microbiology*, 105(1), pp.46–64.

Chandrashekar, R., et al., 1997. Molecular cloning and characterization of a recombinant Histoplasma capsulatum antigen for antibody-based diagnosis of human histoplasmosis. *Journal of clinical microbiology*, 35(5), pp.1071–6.

Conrad, M., et al., 2014. Nutrient sensing and signaling in the yeast Saccharomyces cerevisiae. *FEMS Microbiology Reviews*, 38(2), pp.254–299.

Conway, M.K.,, Grunwald, D., and Heideman, W., 2012. Glucose, nitrogen, and phosphate repletion in saccharomyces cerevisiae: Common transcriptional responses to different nutrient signals. *G3: Genes, Genomes, Genetics*, 2(9), pp.1003–1017.

Creamer, D.R.,, Hubbard, S.J.,, Ashe, M.P., and Grant, C.M., 2022. Yeast Protein Kinase A Isoforms: A Means of Encoding Specificity in the Response to Diverse Stress Conditions? *Biomolecules*, 12(7), p.958.

Davie, J.R., 2003. Inhibition of Histone Deacetylase Activity by Butyrate. *The Journal of Nutrition*, 133(7), pp.2485S-2493S.

Defosse, T.A., et al., 2015. Hybrid histidine kinases in pathogenic fungi. *Molecular Microbiology*, 95(6), pp.914–924.

Dutton, J.R.,, Johns, S., and Miller, B.L., 1997. StuAp is a sequence-specific transcription factor that regulates developmental complexity in Aspergillus nidulans. *The EMBO journal*, 16(18), pp.5710–21.

Edwards, J.A., et al., 2013. Histoplasma yeast and mycelial transcriptomes reveal pathogenic-phase and lineage-specific gene expression profiles. *BMC Genomics 2013 14:1*, 14(1), pp.1–19.

English, B.C., et al., 2017. The transcription factor CHOP, an effector of the integrated stress response, is required for host sensitivity to the fungal intracellular pathogen Histoplasma capsulatum. *PLoS pathogens*, 13(9), p.e1006589.

Fillinger, S., et al., 2002. cAMP and ras signalling independently control spore germination in the filamentous fungus Aspergillus nidulans. *Molecular Microbiology*, 44(4), pp.1001–1016.

Fuller, K.K., et al., 2011. Divergent Protein Kinase A isoforms co-ordinately regulate conidial germination, carbohydrate metabolism and virulence in Aspergillus fumigatus. *Molecular Microbiology*, 79(4), pp.1045–1062.

Fuller, K.K., and Rhodes, J.C., 2012. Protein kinase A and fungal virulence. *https://doi.org/10.4161/viru.19396*, 3(2), pp.109–121.

Garfoot, A.L., et al., 2016. The Eng1 β-Glucanase Enhances Histoplasma Virulence by Reducing β-Glucan Exposure. *mBio*, 7(2), pp.e01388-15.

Gargano, S.,, Di Lallo, G.,, Kobayashi, G.S., and Maresca, B., 1995. A temperature-sensitive strain ofHistoplasma capsulatum has an altered Δ9-fatty acid desaturase geneacid desaturase gene. *Lipids*, 30(10), pp.899–906.

Garreau, H., et al., 2000. Hyperphosphorylation of Msn2p and Msn4p in response to heat shock and the diauxic shift is inhibited by cAMP in Saccharomyces cerevisiae. *Microbiology*, 146(9), pp.2113–2120.

Gasch, A.P., et al., 2000. Genomic expression programs in the response of yeast cells to environmental changes. *Molecular biology of the cell*, 11(12), pp.4241–4257.

Gilmore, S.A.,, Naseem, S.,, Konopka, J.B., and Sil, A., 2013. N-acetylglucosamine (GlcNAc) triggers a rapid, temperature-responsive morphogenetic program in thermally dimorphic fungi. *PLoS Genetics*, 9(9), p.e1003799.

Gilmore, S.A.,, Voorhies, M.,, Gebhart, D., and Sil, A., 2015. Genome-Wide Reprogramming of Transcript Architecture by Temperature Specifies the Developmental States of the Human Pathogen Histoplasma. *PLOS Genetics*, 11(7), p.e1005395.

Glazier, V.E., 2022. EFG1, Everyone's Favorite Gene in Candida albicans: A Comprehensive Literature Review. *Frontiers in Cellular and Infection Microbiology*, 12, p.302.

Görner, W., et al., 1998. Nuclear localization of the C2H2 zinc finger protein Msn2p is regulated by stress and protein kinase A activity.

Harcus, D., et al., 2004. Transcription profiling of cyclic AMP signaling in Candida albicans. *Molecular Biology of the Cell*, 15(10), pp.4490–4499.

Holbrook, E.D., et al., 2014. Glycosylation and immunoreactivity of the Histoplasma capsulatum Cfp4 yeast-phase exoantigen. *Infection and immunity*, 82(10), pp.4414–25.

Holbrook, E.D.,, Smolnycki, K.A.,, Youseff, B.H., and Rappleye, C.A., 2013. Redundant catalases detoxify phagocyte reactive oxygen and facilitate Histoplasma capsulatum pathogenesis. *Infection and immunity*, 81(7), pp.2334–46.

Hwang, L.H.,, Mayfield, J.A.,, Rine, J., and Sil, A., 2008. Histoplasma requires SID1, a member of an iron-regulated siderophore gene cluster, for host colonization. *PLoS pathogens*, 4(4), p.e1000044.

Inglis, D.O.,, Voorhies, M.,, Murray, D.R.H., and Sil, A., 2013. Comparative transcriptomics of infectious spores from the fungal pathogen Histoplasma capsulatum reveals a core set of transcripts that specify infectious and pathogenic states. *Eukaryotic cell*, 12(6), pp.828–852.

Isaac, D.T., et al., 2015. Macrophage cell death and transcriptional response are actively triggered by the fungal virulence factor Cbp1 during H. capsulatum infection. *Molecular microbiology*, 98(5), pp.910–929.

Izawa, M., et al., 2009. Inhibition of histone deacetylase causes reduction of appressorium formation in the rice blast fungus Magnaporthe oryzae. *The Journal of General and Applied Microbiology*, 55(6), pp.489–498.

Johnson, C.H., et al., 2002. Redundancy, phylogeny and differential expression of Histoplasma capsulatum catalases. *Microbiology*, 148(4), pp.1129–1142.

Jorgensen, P., et al., 2004. A dynamic transcriptional network communicates growth potential to ribosome synthesis and critical cell size. *Genes & Development*, 18(20), pp.2491–2505.

Klengel, T., et al., 2005. Fungal adenylyl cyclase integrates CO2 sensing with cAMP signaling and virulence. *Current Biology*, 15(22), pp.2021–2026.

Kujoth, G.C., et al., 2018. CRISPR/Cas9-mediated gene disruption reveals the importance of zinc metabolism for fitness of the dimorphic fungal pathogen Blastomyces dermatitidis. *mBio*, 9(2).

Kunitomo, H.,, Sugimoto, A.,, Yamamoto, M., and Wilkinson, C.R.M., 1995. Schizosaccharomyces pombe pac2 + controls the onset of sexual development via a pathway independent of the cAMP cascade. *Current Genetics*, 28(1), pp.32–38.

Kwon, N.J., et al., 2010. FlbC is a putative nuclear C2H2 transcription factor regulating development in Aspergillus nidulans. *Molecular Microbiology*, 77(5), pp.1203–1219.

Lafon, A., et al., 2005. The heterotrimeric G-protein GanB(α)-SfaD(β)-GpgA(γ) is a carbon source sensor involved in early cAMP-dependent germination in Aspergillus nidulans. *Genetics*, 171(1), pp.71–80.

Lajoie, D.M., and Cordes, M.H.J., 2015. Spider, bacterial and fungal phospholipase D toxins make cyclic phosphate products. *Toxicon*, 108, pp.176–180.

Li, B., and Dewey, C.N., 2011. RSEM: accurate transcript quantification from RNA-Seq data with or without a reference genome. *BMC bioinformatics*, 12, p.323.

Liebmann, B.,, Gattung, S.,, Jahn, B., and Brakhage, A.A., 2003. cAMP signaling in Aspergillus fumigatus is involved in the regulation of the virulence gene pksP and in defense against killing by macrophages. *Molecular genetics and genomics : MGG*, 269(3), pp.420–35.

Liebmann, B.,, Müller, M.,, Braun, A., and Brakhage, A.A., 2004. The cyclic AMP-dependent protein kinase A network regulates development and virulence in Aspergillus fumigatus. *Infection and Immunity*, 72(9), pp.5193–5203.

Longo, L.V.G.,, Ray, S.C.,, Puccia, R., and Rappleye, C.A., 2018. Characterization of the APSES-family transcriptional regulators of Histoplasma capsulatum. *FEMS Yeast Research*, 18(8), p.87.

Maresca, B., et al., 1977. *Regulation of dimorphism in the pathogenic fungus Histoplasma capsulatum [17]. Nature*, .

Marion, C.L.,, Rappleye, C.A.,, Engle, J.T., and Goldman, W.E., 2006. An alpha-(1,4)-amylase is essential for alpha-(1,3)-glucan production and virulence in Histoplasma capsulatum. *Molecular microbiology*, 62(4), pp.970–83.

Martinez-Vazquez, A., et al., 2013. Identification of the Transcription Factor Znc1p, which Regulates the Yeast-to-Hypha Transition in the Dimorphic Yeast Yarrowia lipolytica. *PLOS ONE*, 8(6), p.e66790.

Medoff, J.,, Jacobson, E., and Medoff, G., 1981. Regulation of dimorphism in Histoplasma capsulatum by cyclic adenosine 3',5'-monophosphate. *Journal of Bacteriology*, 145(3), p.1452.

Miller, K.Y.,, Wu, J., and Miller, B.L., 1992. StuA is required for cell pattern formation in Aspergillus. *Genes and Development*, 6(9), pp.1770–1782.

Min, K., et al., 2021. Integrative multi-omics profiling reveals cAMP-independent mechanisms regulating hyphal morphogenesis in Candida albicans. *PLOS Pathogens*, 17(8), p.e1009861.

Minard, K.I., et al., 1998. Sources of NADPH and Expression of Mammalian NADP+-specific Isocitrate Dehydrogenases in Saccharomyces cerevisiae. *Journal of Biological Chemistry*, 273(47), pp.31486–31493.

Nemecek, J.C.,, Wüthrich, M., and Klein, B.S., 2006. Global control of dimorphism and virulence in fungi. *Science*, 312(5773), pp.583–588.

Nguyen, L.N.,, Lopes, L.C.L.,, Cordero, R.J.B., and Nosanchuk, J.D., 2011. Sodium butyrate inhibits pathogenic yeast growth and enhances the functions of macrophages. *Journal of Antimicrobial Chemotherapy*, 66(11), pp.2573–2580.

Nguyen, V.Q., and Sil, A., 2008. Temperature-induced switch to the pathogenic yeast form of Histoplasma capsulatum requires Ryp1, a conserved transcriptional regulator. *Proceedings of the National Academy of Sciences of the United States of America*, 105(12), pp.4880–4885.

Nødvig, C.S.,, Nielsen, J.B.,, Kogle, M.E., and Mortensen, U.H., 2015. A CRISPR-Cas9 System for Genetic Engineering of Filamentous Fungi. *PLOS ONE*, 10(7), p.e0133085.

Pan, X., and Heitman, J., 1999. Cyclic AMP-Dependent Protein Kinase Regulates Pseudohyphal Differentiation in Saccharomyces cerevisiae . *Molecular and Cellular Biology*, 19(7), pp.4874–4887.

Pan, X., and Heitman, J., 2002. Protein Kinase A Operates a Molecular Switch That Governs Yeast Pseudohyphal Differentiation. *Molecular and Cellular Biology*, 22(12), pp.3981–3993.

Parrino, S.M., et al., 2017. cAMP-independent signal pathways stimulate hyphal morphogenesis in Candida albicans. *Molecular Microbiology*, 103(5), pp.764–779.

Pfaller, M.A., and Diekema, D.J., 2010. Epidemiology of Invasive Mycoses in North America. *http://dx.doi.org/10.3109/10408410903241444*, 36(1), pp.1–53.

Pidroni, A., et al., 2018. A class 1 histone deacetylase as major regulator of secondary metabolite production in Aspergillus nidulans. *Frontiers in Microbiology*, 9(SEP), p.2212.

Polley, S.D., and Caddick, M.X., 1996. Molecular characterisation of meaB, a novel gene affecting nitrogen metabolite repression in Aspergillus nidulans. *FEBS Letters*, 388(2–3), pp.200–205.

Ritchie, M.E., et al., 2015. limma powers differential expression analyses for RNA-sequencing and microarray studies. *Nucleic acids research*, 43(7), p.e47.

Rocha, C.R.C., et al., 2001. Signaling through adenylyl cyclase is essential for hyphal growth and virulence in the pathogenic fungus Candida albicans. *Molecular Biology of the Cell*, 12(11), pp.3631–3643.

Rodriguez, L., et al., 2019. Opposing signaling pathways regulate morphology in response to temperature in the fungal pathogen Histoplasma capsulatum. *PLoS biology*, 17(9), p.e3000168.

Sacco, M., et al., 1981. Temperature- and cyclic nucleotide-induced phase transitions of Histoplasma capsulatum. *Journal of bacteriology*, 146(1), pp.117–20.

Saputo, S.,, Kumar, A., and Krysan, D.J., 2014. Efg1 directly regulates ACE2 expression to mediate cross talk between the cAMP/PKA and RAM pathways during candida albicans morphogenesis. *Eukaryotic Cell*, 13(9), pp.1169–1180.

Scherr, G.H., 1957. Studies on the dimorphism of Histoplasma capsulatum: I. The roles of -SH groups and incubation temperature. *Experimental Cell Research*, 12(1), pp.92–107.

Sebghati, T.S.,, Engle, J.T., and Goldman, W.E., 2000. Intracellular parasitism by Histoplasma capsulatum: fungal virulence and calcium dependence. *Science (New York, N.Y.)*, 290(5495), pp.1368–72.

Sewall, T.C.,, Mims, C.W., and Timberlake, W.E., 1990. Conidium differentiation in Aspergillus nidulans wild-type and wet-white (wetA) mutant strains. *Developmental Biology*, 138(2), pp.499–508.

Sheppard, D.C., et al., 2005. The Aspergillus fumigatus StuA protein governs the up-regulation of a discrete transcriptional program during the acquisition of developmental competence. *Molecular biology of the cell*, 16(12), pp.5866–79.

Shimizu, K., and Keller, N.P., 2001. Genetic involvement of a cAMP-dependent protein kinase in a G protein signaling pathway regulating morphological and chemical transitions in Aspergillus nidulans. *Genetics*, 157(2), pp.591–600.

Shwab, E.K., et al., 2007. Histone deacetylase activity regulates chemical diversity in Aspergillus. *Eukaryotic Cell*, 6(9), pp.1656–1664.

Smith, A.,, Ward, M.P., and Garrett, S., 1998. Yeast PKA represses Msn2p/Msn4p-dependent gene expression to regulate growth, stress response and glycogen accumulation. *The EMBO Journal*, 17(13), pp.3556–3564.

Smyth, G.K., 2004. Linear models and empirical bayes methods for assessing differential expression in microarray experiments. *Statistical applications in genetics and molecular biology*, 3, p.Article3.

Sonneborn, A., et al., 2000. Protein kinase A encoded by TPK2 regulates dimorphism of Candida albicans. *Molecular Microbiology*, 35(2), pp.386–396.

Stoldt, V.R.,, Sonneborn, A.,, Leuker, C.E., and Ernst, J.F., 1997. Efg1p, an essential regulator of morphogenesis of the human pathogen Candida albicans, is a member of a conserved class of bHLH proteins regulating morphogenetic processes in fungi. *EMBO Journal*, 16(8), pp.1982–1991.

Storlazzi, A.,, Maresca, B., and Gargano, S., 1999. cAMP Is Involved in Transcriptional Regulation of Δ9-Desaturase during Histoplasma capsulatum Morphogenesis. *Molecular Cell Biology Research Communications*, 2(3), pp.172–177.

Thevelein, J.M., and de Winde, J.H., 1999. Novel sensing mechanisms and targets for the cAMP-protein kinase A pathway in the yeast Saccharomyces cerevisiae. *Molecular Microbiology*, 33(5), pp.904–918.

Thieme, K.G., et al., 2018. Velvet domain protein VosA represses the zinc cluster transcription factor SclB regulatory network for Aspergillus nidulans asexual development, oxidative stress response and secondary metabolism. *PLoS genetics*, 14(7).

Thomas, D.,, Cherest, H., and Surdin-Kerjan, Y., 1991. Identification of the structural gene for glucose-6-phosphate dehydrogenase in yeast. Inactivation leads to a nutritional requirement for organic sulfur. *The EMBO Journal*, 10(3), pp.547–553.

Vienken, K., and Fischer, R., 2006a. The Zn(II)2Cys6 putative transcription factor NosA controls fruiting body formation in Aspergillus nidulans. *Molecular Microbiology*, 61(2), pp.544–554.

Vienken, K., and Fischer, R., 2006b. The Zn(II)2Cys6 putative transcription factor NosA controls fruiting body formation in Aspergillus nidulans. *Molecular Microbiology*, 61(2), pp.544–554.

Webster, R.H., and Sil, A., 2008. Conserved factors Ryp2 and Ryp3 control cell morphology and infectious spore formation in the fungal pathogen Histoplasma capsulatum. *Proceedings of the National Academy of Sciences of the United States of America*, 105(38), pp.14573–14578.

de Wever, V., et al., 2005. A dual role for PP1 in shaping the Msn2-dependent transcriptional response to glucose starvation. *The EMBO Journal*, 24(23), pp.4115–4123.

Youseff, B.H.,, Holbrook, E.D.,, Smolnycki, K.A., and Rappleye, C.A., 2012. Extracellular superoxide dismutase protects Histoplasma yeast cells from host-derived oxidative stress. *PLoS pathogens*, 8(5), p.e1002713.

Zamith-Miranda, D., et al., 2021. A Histoplasma capsulatum Lipid Metabolic Map Identifies Antifungal Targets. *mBio*, 12(6), p.e0297221.

Zutz, C., et al., 2013. Small Chemical Chromatin Effectors Alter Secondary Metabolite Production in Aspergillus clavatus. *Toxins*, 5(10), p.1723.

Publishing Agreement

It is the policy of the University to encourage open access and broad distribution of all theses, dissertations, and manuscripts. The Graduate Division will facilitate the distribution of UCSF theses, dissertations, and manuscripts to the UCSF Library for open access and distribution. UCSF will make such theses, dissertations, and manuscripts accessible to the public and will take reasonable steps to preserve these works in perpetuity.

I hereby grant the non-exclusive, perpetual right to The Regents of the University of California to reproduce, publicly display, distribute, preserve, and publish copies of my thesis, dissertation, or manuscript in any form or media, now existing or later derived, including access online for teaching, research, and public service purposes.

DocuSigned by:

DAFC2BB4500A4B0...

Author Signature

12/6/2022

Date